Pre-B cell receptor acts as a selectivity switch for galectin-1 at the pre-B cell surface

Pauline Touarin, Bastien Serrano, Audrey Courbois, Olivier Bornet, Qian Chen, Lincoln G Scott, James R Williamson, Corinne Sebban-Kreuzer, Stéphane J.C. Mancini, Latifa Elantak

Cell Reports

Article

Pre-B cell receptor acts as a selectivity switch for galectin-1 at the pre-B cell surface

Graphical abstract

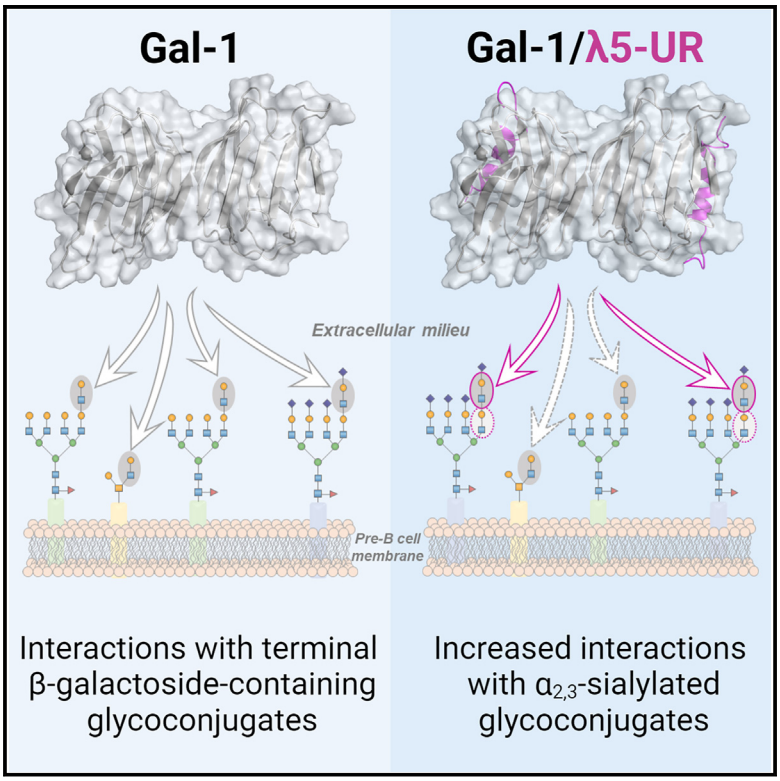

Highlights

- The pre-BCR (λ5-UR) modifies Gal-1 binding to cell surface glycoconjugates
- Gal-1 targets cell surface α2,3-sialylated glycoconjugates upon pre-BCR binding
- Gal-1 selectivity switch occurs by increased contacts with α2,3-sialylated glycans
- Targeting of α2,3-sialylated glycoconjugates by Gal-1 regulates pre-BCR signaling

Authors

Pauline Touarin, Bastien Serrano, Audrey Courbois, ..., Corinne Sebban-Kreuzer, Stéphane J.C. Mancini, Latifa Elantak

Correspondence

elantak@imm.cnrs.fr

In brief

Touarin et al. report NMR monitoring of Gal-1 binding to cell surface ligands. They find that interaction with the pre-BCR changes Gal-1 binding to specifically target α2,3-sialylated glycoconjugates at the pre-B cell surface. This targeting regulates pre-BCR signaling, a key checkpoint during B cell development.

Touarin et al., 2024, Cell Reports *43*, 114541
August 27, 2024
https://doi.org/10.1016/j.celrep.2024.114541

CellPress

Cell Reports

CellPress
OPEN ACCESS

Article

Pre-B cell receptor acts as a selectivity switch for galectin-1 at the pre-B cell surface

Pauline Touarin,[1] Bastien Serrano,[1] Audrey Courbois,[1] Olivier Bornet,[2] Qian Chen,[3] Lincoln G. Scott,[3] James R. Williamson,[4] Corinne Sebban-Kreuzer,[1] Stéphane J.C. Mancini,[5,6] and Latifa Elantak[1,6,7,*]

[1]Laboratoire d'Ingénierie des Systèmes Macromoléculaires (LISM UMR7255), Institut de Microbiologie de la Méditerranée, Institut de Microbiologie, Bioénergies et Biotechnologies, CNRS, Aix-Marseille University, Marseille, France
[2]NMR platform, Institut de Microbiologie de la Méditerranée (IMM FR3479), Institut de Microbiologie, Bioénergies et Biotechnologies, CNRS, Aix-Marseille University, Marseille, France
[3]Cassia, 3030 Bunker Hill Street, Suite 214, San Diego, CA 92109, USA
[4]Department of Integrative Structural and Computational Biology, The Scripps Research Institute, La Jolla, CA 92037, USA
[5]University Rennes, INSERM, EFS, UMR S1236, Rennes, France
[6]Senior author
[7]Lead contact
*Correspondence: elantak@imm.cnrs.fr
https://doi.org/10.1016/j.celrep.2024.114541

SUMMARY

Galectins are glycan-binding proteins translating the sugar-encoded information of cellular glycoconjugates into physiological activities, including immunity, cell migration, and signaling. Galectins also interact with non-glycosylated partners in the extracellular milieu, among which the pre-B cell receptor (pre-BCR) during B cell development. How these interactions might interplay with the glycan-decoding function of galectins is unknown. Here, we perform NMR experiments on native membranes to monitor Gal-1 binding to physiological cell surface ligands. We show that pre-BCR interaction changes Gal-1 binding to glycosylated pre-B cell surface receptors. At the molecular and cellular levels, we identify α2,3-sialylated motifs as key targeted epitopes. This targeting occurs through a selectivity switch increasing Gal-1 contacts with α2,3-sialylated poly-*N*-acetyllactosamine upon pre-BCR interaction. Importantly, we observe that this switch is involved in the regulation of pre-BCR activation. Altogether, this study demonstrates that interactions to non-glycosylated proteins regulate the glycan-decoding functions of galectins at the cell surface.

INTRODUCTION

Glycans are essential for life and play many different fundamental roles in nearly all biological processes.[1] Their tremendous diversity is key to store chemical information at the cell surfaces—glycocode—which is translated into cellular responses by binding to specific proteins mainly known as lectins.[2,3] Among lectins, galectins are a highly conserved family of 15 known proteins (Gal-1 to Gal-15), defined by their ability to bind β-galactosides through a conserved carbohydrate recognition domain (CRD) which includes the carbohydrate binding site (CBS).[4] These lectins, found in many cell types,[5] are well-known regulators of cell responses and mediate a wide variety of functions such as cell binding, migration, differentiation, cellular trafficking, and cell signaling.[4] Galectins are also involved in several pathological processes such as inflammatory diseases, oncogenesis, cardiovascular disorders, and host-pathogen interactions,[6–10] making galectins attractive therapeutic targets.[11–13] All these functions, at the surface of many different cell types, in all kind of environments, are achieved through their ability to oligomerize, which leads to crosslinking of specific cell-surface glycoproteins or glycolipids into lattices.[14] Given the abundance of β-galactoside-derived glycoconjugates on cell surfaces, how these lectins select a subset of ligands among many available candidates to mediate a specific cellular function remains elusive.

The concept of galectins as functioning in the extracellular compartment only through carbohydrate interactions has been challenged recently by the identification of non-glycosylated binding partners.[15–20] Whether these interactions participate in cell glycome decoding by galectins is unknown. The first example of a carbohydrate-independent interaction in the extracellular compartment concerns the prototype Gal-1 homodimer and the pre-B cell receptor (pre-BCR).[21] Gal-1 is an exo-type lectin (i.e., it interacts specifically with terminal units of polysaccharides).[22,23] During B cell differentiation in the bone marrow, pre-BCRs are expressed at the surface of pre-B cells, which are present in a specialized cellular niche consisting of stromal cells secreting Gal-1. At this developmental stage, Gal-1 establishes interactions with glycoconjugates and the pre-BCRs at the contact zone between pre-B and stromal cells.[21,24,25] This Gal-1-dependent lattice drives pre-BCR clustering, activation, and subsequent downstream signaling, which has been implicated in cell survival, proliferation, and differentiation.[26] However, the

molecular mechanism underlying Gal-1 functions at the pre-B cell surface remains unknown. Our previous study revealed that Gal-1 interacts with a non-glycosylated region of the pre-BCR, the λ5 unique region (λ5-UR), that docks onto a Gal-1 hydrophobic surface behind the CBS.[27] While binding at a distance from the CBS, λ5-UR induces carbohydrate affinity changes as tested on glycan arrays.[15] These data suggested that λ5-UR binding to Gal-1 modulates Gal-1 binding activity for structurally related carbohydrates. Whether these affinity changes represent a mechanism to regulate Gal-1 interactions and function at the pre-B cell surface is still to be demonstrated on physiological cell surface ligands embedded in the plasma membrane. To date there are no published data analyzing at the structural level galectin binding to native cell surface ligands.

Here, we addressed the challenge of studying Gal-1 binding to pre-B and stromal cell surfaces using solution-state NMR spectroscopy on native membranes and investigated the effect of λ5-UR interaction on Gal-1 binding to its physiological ligands. We show that λ5-UR allows Gal-1 to select specific glycosylated receptors at the pre-B cell surface. We identified α2,3-sialylated glycans as key targeted epitopes. Defining the structural basis of this regulation highlighted increased Gal-1 intermolecular contacts with α2,3-sialylated poly-*N*-acetyllactosamine upon λ5-UR interaction, which regulates pre-BCR activation. Altogether, our study shows that galectin/non-glycosylated protein interactions can act as regulators of galectin functions and may be the missing piece of the puzzle to understand how galectins acquire their target specificity at the cell surface.

RESULTS

Structural basis of Gal-1 binding to cell surface ligands

To investigate Gal-1 binding to glycoconjugates in their native membrane environment, we utilized stromal and pre-B cell lines (OP9 and Nalm6, respectively) to extract glycoconjugates-enriched membrane vesicles amenable for NMR studies. These cell lines were previously used to model the pre-B/stromal cell synapse and pre-BCR relocalization.[27] For reference, we observed on average 50- and 25-nm diameter vesicles extracted from stromal and pre-B cell lines, respectively (Figure S1A and S1B). These vesicles were previously used to investigate the glycomic profile of pre-B and stromal cell lines and have been shown to bind to Gal-1.[15] NMR experiments carried out consisted of recording ^{1}H,^{15}N heteronuclear single quantum coherence (HSQC) spectra on ^{15}N-labeled Gal-1 alone and incubated with membrane vesicles (Figure 1A). Importantly, as we are working with native membranes, it is not possible to evaluate the exact cell surface concentration of Gal-1 ligands. In our protocol, we evaluate the total amount of proteins (glycosylated or not) contained in the cell vesicle samples to have a "cursor" for experimental reproducibility. Ultimately, Gal-1 ligands concentrations are most likely lower compared to the ^{15}N-labeled Gal-1 used in these experiments. Furthermore, to prevent endogenous Gal-1 from stromal cells to interfere with added ^{15}N-Gal-1, we used stromal cells for which Gal-1 expression has been decreased.[28] Upon vesicle addition, chemical shift deviations (CSDs) and line broadening were observed, indicative of complex formation with vesicle surface ligands (Figures 1A, 1B,S1C, and S1D). To provide evidence that glycans mediate Gal-1 binding to cell vesicles, we enzymatically cleaved complex N-glycans, as well as core1 and core3 O-glycans, from the cell surface glycoproteins using peptide-N-glycosidase F (PNGase F) and O-glycosidase. After treatment, no significant variation or intensity decrease was observed on Gal-1 spectra, confirming that Gal-1 interaction to cell vesicles is glycan dependent (Figure S1E). These results demonstrate not only the presence of functional glycosylated ligands in the isolated membrane vesicles but also the possibility to monitor Gal-1 interactions at atomic resolution in their physiological context.

Remarkably, Gal-1 resonances presenting perturbations are localized in the CBS but also at the edge of Gal-1 β sheet (Figures 1C and 1D). Previously, the Gal-1 CBS had been defined as containing five subsites, A–E, where subsite C accommodates the essential β-galactose unit, the other subsites interacting more specifically with the other units of the glycan.[30] When incubated with cell vesicles, CBS subsites C and D were mainly perturbed, thus confirming Gal-1 binding to cell surface β-galactosides (Figures 1C and 1D). However, significant differences were observed at the residue level within these subsites depending on the cell vesicles added. Remarkably, additional perturbations in CBS subsites A and B were observed in the presence of stromal cell vesicles, indicating binding to β-galactoside ligands with extensions pointing toward these subsites (Figure 1D). In addition to CBS perturbations, residues at the edge of Gal-1 β sheets next to the CBS also showed strong resonance perturbations (Figures 1C and 1D). These variations outside the CBS could represent an additional interaction site for extended complex cellular glycans. Finally, residues at the dimer interface also showed resonance perturbations, which is consistent with previous studies demonstrating the long-range effects of glycan binding to galectins.[31–35] Altogether, these data show that Gal-1 binding to cell surface glycosylated ligands impact not only the CBS but also other regions of the CRD. Ultimately, although β-galactose is the main Gal-1-binding determinant, significant differences are also observed at the residue level demonstrating that pre-B and stromal cells contain different sets of Gal-1 ligands. These results are in agreement with lectin microarray data on pre-B and stromal cells showing cell-specific glycomic signatures.[15]

λ5-UR changes Gal-1 binding to pre-B and stromal cell ligands

Within the pre-B cell niche, Gal-1 secreted by stromal cells contacts pre-B cells through binding to glycosylated receptors and to λ5-UR from the pre-BCR.[21,24] To determine whether λ5-UR can change Gal-1 binding properties to cell glycosylated ligands, we examined the effect of λ5-UR on the resulting ^{1}H, ^{15}N-HSQC spectra of Gal-1 in the presence of pre-B or stromal cell vesicles (Figures S2A and S3A).

When added to Gal-1 bound to pre-B cell vesicles, λ5-UR induced CSDs in the λ5-UR binding site and within the CBS (Figures 2A, 2B, and S2A). Remarkably, several of the resonances already affected by pre-B vesicle interaction shifted in the opposite direction toward their initial Gal-1 free resonance position (Figure 2C) upon λ5-UR binding. These resonances belong to CBS subsites C and D. Final calculated CSDs

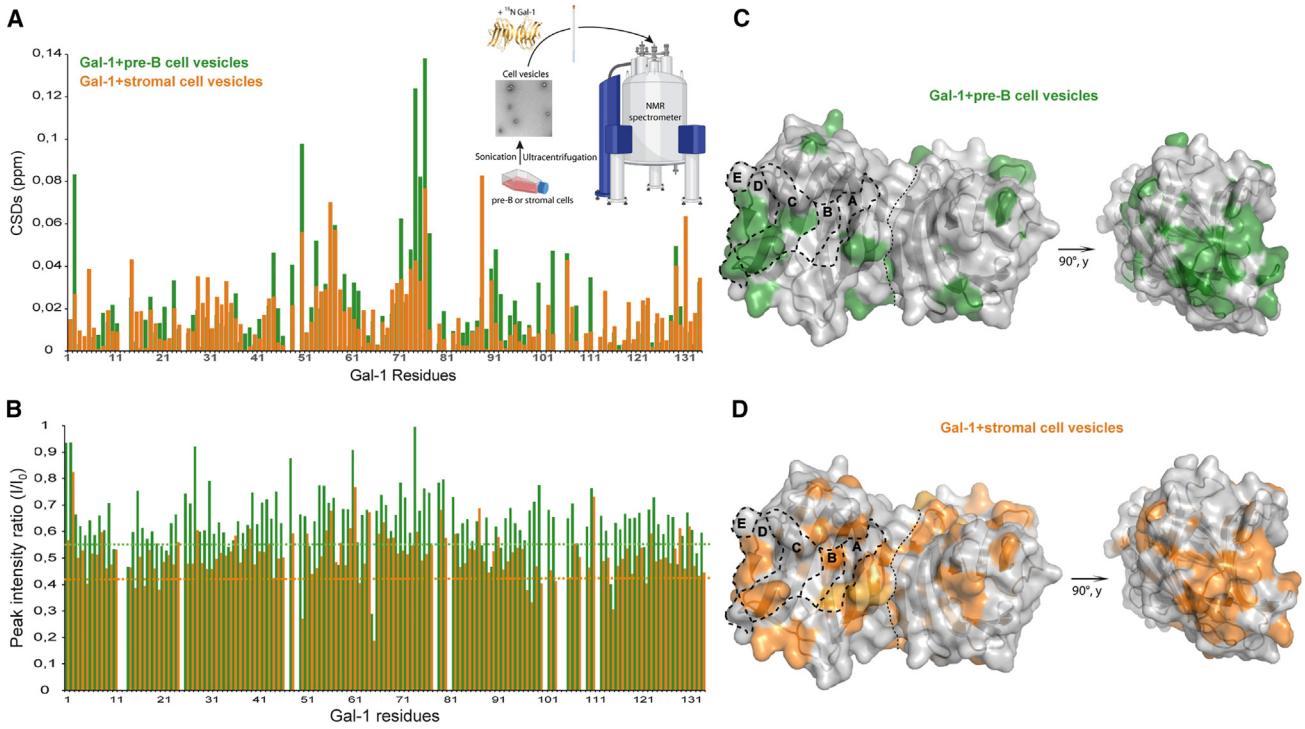

Figure 1. Gal-1 binding to pre-B and stromal cell surface ligands

(A) A histogram showing CSDs upon addition into a ^{15}N-labeled Gal-1 sample of membrane vesicles extracted from 100 million pre-B cells (green bars) and 10 million stromal cells (orange bars). At top right, the strategy for NMR study of Gal-1 binding to pre-B and stromal cell vesicles is depicted. Cells are cultured as described in the Method details section and then sonicated to generate the vesicles, which are collected after the ultracentrifugation cycles. Vesicles are finally incubated with ^{15}N-labeled Gal-1 to proceed to NMR experiment recording.

(B) Normalized peak intensity ratio analysis (I/I_0) of Gal-1 bound to pre-B (green bars) or stromal (orange bars) cell vesicles relative to unbound Gal-1. Dotted lines represent 1σ from the average I/I_0.

(C and D) Residues whose resonances have considerable CSDs and peak intensity decrease upon (C) pre-B and (D) stromal vesicles addition are mapped onto a Gal-1 homodimer surface structure (PDB: 1GZW[29]). (Left) The CBS view. (Right) The side view after a 90° rotation. CBS subsites are framed and labeled on one monomer (only one CBS is entirely visible due to the homodimer symmetry).

(comparison between Gal-1 free and Gal-1 bound to pre-B cell vesicles and λ5-UR) for these resonances decreased until complete cancellation at a 1:3 Gal-1:λ5-UR ratio (Figure S2B). These observations indicate that pre-B cell ligands of Gal-1 are counter-selected in the presence of λ5-UR. Then, upon increasing λ5-UR addition, other CBS resonances located in CBS subsites B and C and in loops surrounding the CBS started to shift (Figures 2C and S2B). In addition to CSDs, signal intensities were modified upon λ5-UR interaction (Figure 2D). Specifically, both increased (subsite D and surrounding loops) and decreased peak intensities (subsite C) were observed (Figure 2D), which further support changes in Gal-1 binding to cell vesicles. Consequently, the final binding pattern of Gal-1 to pre-B cell vesicles is different in the presence of λ5-UR, indicating binding to new ligands (Figure 1C vs. Figure 2E). A control peptide, λ5-UR mutated on two essential residues for complex formation with Gal-1 (λ5-UR-L26A-W30A),[27] has been used to verify that the effect observed is specific to λ5-UR binding to Gal-1. No CSDs were observed with the mutated peptide (Figures 2A and S2C). Collectively, these experiments demonstrate glycan-binding changes for Gal-1 at the pre-B cell surface upon λ5-UR interaction, decreasing affinity for some glycan epitopes and enhancing interaction with others, thus maintaining Gal-1 association with the pre-B cell surface.

In the presence of stromal cell vesicles, λ5-UR induces CSDs and a strong decrease in Gal-1 NMR signals (Figures S3A–S3C). Here, perturbations behavior is different compared to the same experiment in the presence of pre-B cell vesicles. Indeed, the perturbations already observed in the presence of stromal cell vesicles are increased and extended upon λ5-UR addition, indicative of a peptide-induced enhancement of Gal-1 interactions. Combined analysis of CSDs and peak intensity decrease highlighted perturbations for resonances located mainly in the CBS and at the edge of Gal-1 β sheets, including residues belonging to the λ5-UR binding site (Figure S3D). In the absence of cell vesicles, λ5-UR alone is not able to prompt such a Gal-1 signal intensity decrease, which is consistent with the binding of a 24-amino acid peptide in the fast exchange regime.[27] Therefore, λ5-UR interaction induces variations within the CBS, resulting in Gal-1-enhanced binding to stromal cell surface glycans.

In summary, while the addition of the λ5-UR interacting region induces perturbations of Gal-1 resonances, the perturbations observed are different depending on the cell vesicles bound to

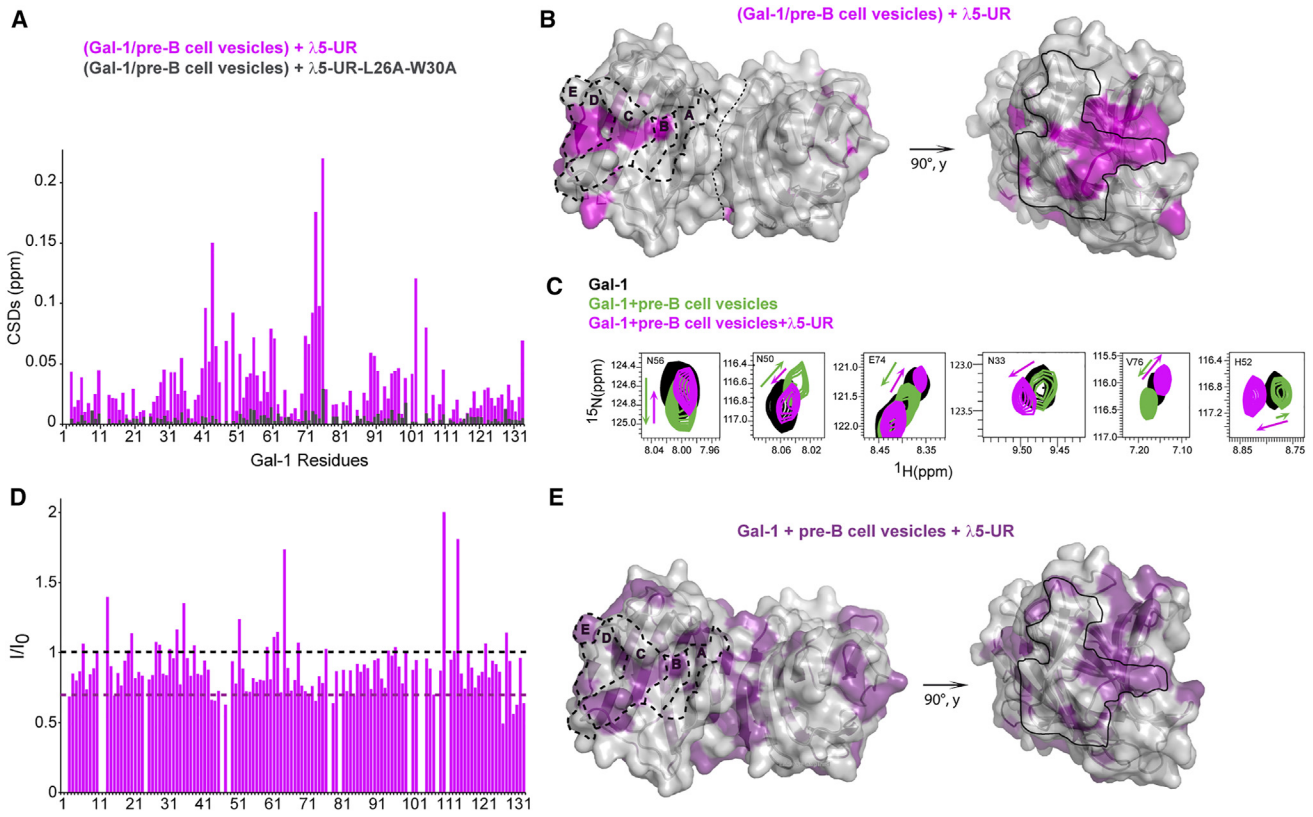

Figure 2. Impact of λ5-UR interaction on Gal-1 binding to pre-B cell vesicles

(A) A histogram showing CSDs of Gal-1 resonances bound to pre-B cell vesicles upon addition of 4.5 M equivalent of λ5-UR (magenta bars) and λ5-UR-L26A-W30A (gray bars).

(B) CSDs are reported on the Gal-1 surface (magenta). The λ5-UR binding site is framed (black line).

(C) Chemical shift perturbations of selected Gal-1 resonances upon addition of pre-B cell vesicles (green) followed by λ5-UR addition (magenta). N56, N50, E74, and V76 resonances show chemical shift perturbations in the presence of pre-B cell vesicles but move back toward their initial Gal-1 free resonance position upon λ5-UR addition. N33 and H52 resonances show increased perturbations upon λ5-UR interaction while being part of the CBS and not the λ5-UR binding site.

(D) Normalized peak intensity ratio analysis (I/I_0) of Gal-1 bound to pre-B cell vesicles and λ5-UR (I) relative to Gal-1 bound to pre-B cell vesicles only (I_0). Dotted magenta line represents 1σ from the average I/I_0. Bars above 1 are indicative of increased peak intensity upon λ5-UR interaction.

(E) Combined chemical shift perturbations (CSDs and I/I_0) between Gal-1 free and Gal-1 bound to pre-B cell vesicles and λ5-UR are reported on Gal-1 homodimer surface structure (purple).

Gal-1. Consequently, λ5-UR can regulate differentially the binding properties of Gal-1 to stromal and pre-B cell surface ligands.

Specific dynamic changes mediate λ5-UR-induced Gal-1 regulation

The λ5-UR binding on Gal-1 backside is transmitted to the CBS to target specific glycoconjugates, and therefore regulates Gal-1 interactions in an allosteric manner. Allostery involves the coupling of ligand binding at one site with a conformational or dynamic change at a distant site, thereby affecting binding at that site. No structural changes within the Gal-1 CBS that could explain enhanced interaction with glycans had been observed upon the binding of λ5-UR[27]; hence, we investigated the role of dynamics in the regulation of Gal-1 interactions mediated by λ5-UR. The backbone dynamics of Gal-1 were analyzed using nuclear spin relaxation parameters for Gal-1 free and bound to λ5-UR (Figures S4A and S4B). The role of fast protein motions was determined by measuring changes in the order parameter S^2. S^2 is a measure of the amplitude of internal motions on the picosecond-to-nanosecond timescale and can vary from $S^2 = 1$, for a bond vector with no internal motion, to $S^2 = 0$, for a bond vector that is rapidly sampling multiple orientations.[36] λ5-UR binding to Gal-1 caused a large number of residues to decrease their motions as evidenced by the corresponding increase in their S^2 values (Figure S5A). More specifically, λ5-UR binding to Gal-1 resulted in line broadening and increased rigidity (increased S^2) for residues from the λ5-UR binding site but also for residues from the upper loop of the CBS subsite C and within subsite D and B (Figure S5C). By contrast, increased flexibility (decreased S^2) was observed for the lower loop of the CBS subsite C. It should be noted that chemical shift analysis showed that λ5-UR binding to Gal-1 in the presence of pre-B cell vesicles (Figure 2F) elicited changes in chemical shift for resonances precisely located within the same regions. The same experiments performed using the anginex synthetic peptide, known to interact with Gal-1 and to induce glycan binding changes,[37,38]

revealed that contrary to λ5-UR, anginex induces a widespread decrease in S^2, indicating a global increase in protein flexibility (Figures S4C, S5B, and S5D). Consequently, the dynamic changes observed upon λ5-UR binding appear to be specific to the λ5-UR protein sequence and may contribute to glycan specificity changes observed toward pre-B and stromal cell surface ligands.

λ5-UR regulates binding of Gal-1 by selecting α2,3-sialylated glycan motifs found on pre-B cell surfaces

Our previous glycome exploration of pre-B and stromal cells highlighted a glycomic signature specific to pre-B cells corresponding to biantennary N-glycans, sulfated-, and α2,3-sialylated β-galactoside glycans.[15] Importantly, the latter showed increased binding to Gal-1 on glycan arrays in the presence of λ5-UR.[15] In addition, sialylated glycans have been shown to be involved in immunologic processes.[39,40] We therefore hypothesized that α2,3-sialylated glycans could be one of the specific glycosidic epitopes targeted by Gal-1 at the pre-B cell surface upon λ5-UR interaction. To test this hypothesis, pre-B cells were treated with neuraminidase S enzyme, which catalyzes the hydrolysis of α2-3-linked *N*-acetylneuraminic acid residues from glycoproteins and oligosaccharides. Cell vesicles generated from the treated cells were incubated with ^{15}N-labeled Gal-1 to analyze Gal-1/vesicles interaction using NMR. After neuraminidase treatment, Gal-1 is still able to bind to the vesicles (Figures 3A and 3B) and show greater interaction compared to untreated ones (higher CSDs and signal intensity decrease). This result indicates that α2,3-sialylation removal revealed glycan motifs for which Gal-1 presents a greater interaction. Remarkably, the addition of λ5-UR induces weaker CSDs compared to the same experiment without neuraminidase treatment (Figure 3C). In addition, signal intensities analysis shows an overall weaker decrease in the presence of λ5-UR after the removal of α2,3-sialylation from pre-B cell vesicles compared to untreated vesicles, and numerous resonances display increased intensity ($I/I_0 > 1$) (Figure 3D). Therefore, these results demonstrate that λ5-UR interaction does not have the same effect on Gal-1 binding to cell vesicles after removal of α2,3-sialyl moieties compared to untreated vesicles. Moreover, signal intensity increase upon λ5-UR interaction suggests decreased Gal-1 binding to treated pre-B cell vesicles.

To further confirm these findings on live pre-B cells, Gal-1 binding has been assessed using flow cytometry (Figure 3E). Gal-1 incubation with pre-B cells showed significant cell surface binding, and the complete loss of Gal-1 binding upon lactose treatment demonstrates that most of it was related to the interaction with glycosylated proteins (Figure 3E). Remarkably, Gal-1 binding at the cell surface was significantly higher following neuraminidase treatment (Figure 3E), as observed by NMR using treated pre-B cell vesicles (Figures 3A and 3B). Binding to higher-affinity ligands is also illustrated by the fact that lactose, a low-affinity ligand, is not able to abolish Gal-1 binding as seen with untreated cells. Despite this increased binding of Gal-1 to treated cells, the addition of λ5-UR induces decreased Gal-1 binding, whereas there is no significant difference in Gal-1 binding to untreated cells in the presence of λ5-UR (Figure 3E). These results suggest that Gal-1 binding to ligands containing α2,3-sialyl moieties is specifically regulated by λ5-UR interaction at the pre-B cell surface.

To validate this specific regulation, we performed an additional assay on live cells without glycome modification. In this assay, pre-B cells were incubated with the *Maackia amurensis* lectin II (MAL II) lectin, which specifically recognizes α2,3-sialylated glycans and is thus expected to antagonize Gal-1 binding to pre-B cells in the presence of λ5-UR. Remarkably, when incubated with MAL II, cells showed a strong loss in viability (Figure 4A), indicating that the interaction of MAL II with the broad range of α2,3-sialylated receptors at the pre-B cell surface triggers a signaling pathway leading to cell death (Figure 4B). Neither Gal-1 nor λ5-UR reversed the induction of cell death by MAL II, thus illustrating their individual inability to perturb MAL II interactions with α2,3-sialylated receptors (Figures 4A and 4C). However, when Gal-1 is combined with λ5-UR, the MAL II-induced cell death was significantly inhibited (Figure 4A). In addition, cell surface binding of Gal-1 was assessed and showed that Gal-1 was bound to pre-B cell surfaces in the presence of MAL II in a carbohydrate-dependent manner (Figure 4E). These observations demonstrate that λ5-UR binding to Gal-1 provokes increased affinity for α2,3-sialylated receptors containing β-galactosides, perturbing MAL II network interactions and precluding cell death signaling (Figure 4D). Of note, in the absence of MAL II, Gal-1, λ5-UR, or a combination of both are unable to induce strong pre-B cell death as seen with MAL II (Figure 4A). Altogether, these results demonstrate that λ5-UR mediates Gal-1-specific targeting of ligands containing α2,3-sialyl moieties at the pre-B cell surface. The structural basis of such ligand-binding selection remains to be unraveled.

λ5-UR induces increased Gal-1 contacts with α2,3-sialylated di-LacNAc

To further investigate at atomic resolution the effect of λ5-UR on the Gal-1/α2,3-sialylated glycan interaction, we synthesized using a chemo-enzymatic-based methodology the α2,3-sialyl di-LacNAc pentasaccharide called hereafter SdiLN (Figure S6A). Since galactose moieties are essential to Gal-1 binding, we also synthesized the pentasaccharide fully ^{13}C labeled on the galactose moieties (Figure S6B). We tested its interaction with Gal-1 using saturation transfer difference (STD) NMR spectroscopy. This technique is based on the selective irradiation of protein protons and subsequent detection of magnetization transfer to small ligands.[42,43] In the presence of Gal-1, magnetization transfer was observed, indicating intermolecular contacts with the pentasaccharide (Figure 5A). The STD signal arises mainly from interaction with the terminal galactose (Gal_A), as expected for an exo-type lectin (Figures 5A and S7A). In addition, ^{1}H,^{13}C-HSQC spectra recorded before and after the addition of Gal-1 to the ^{13}C-labeled SdiLN showed severe peak loss for Gal_A, which is therefore the core binding unit to Gal-1 (Figures 5B and 5C). These data are consistent with the Gal-1 classification as an exo-type lectin.[44,45] The reverse experiment, where Gal-1 is ^{15}N labeled and the SdiLN is unlabeled has also been performed and showed CSDs and decreased peak intensities mainly for Gal-1 resonances located in CBS subsite C, where the core binding galactose Gal_A of the SdiLN is likely interacting (Figures 5D,S7C, and S7D).

Surprisingly, in the presence of λ5-UR, STD signal contributions became equivalent for Gal_A and Gal_B, demonstrating that

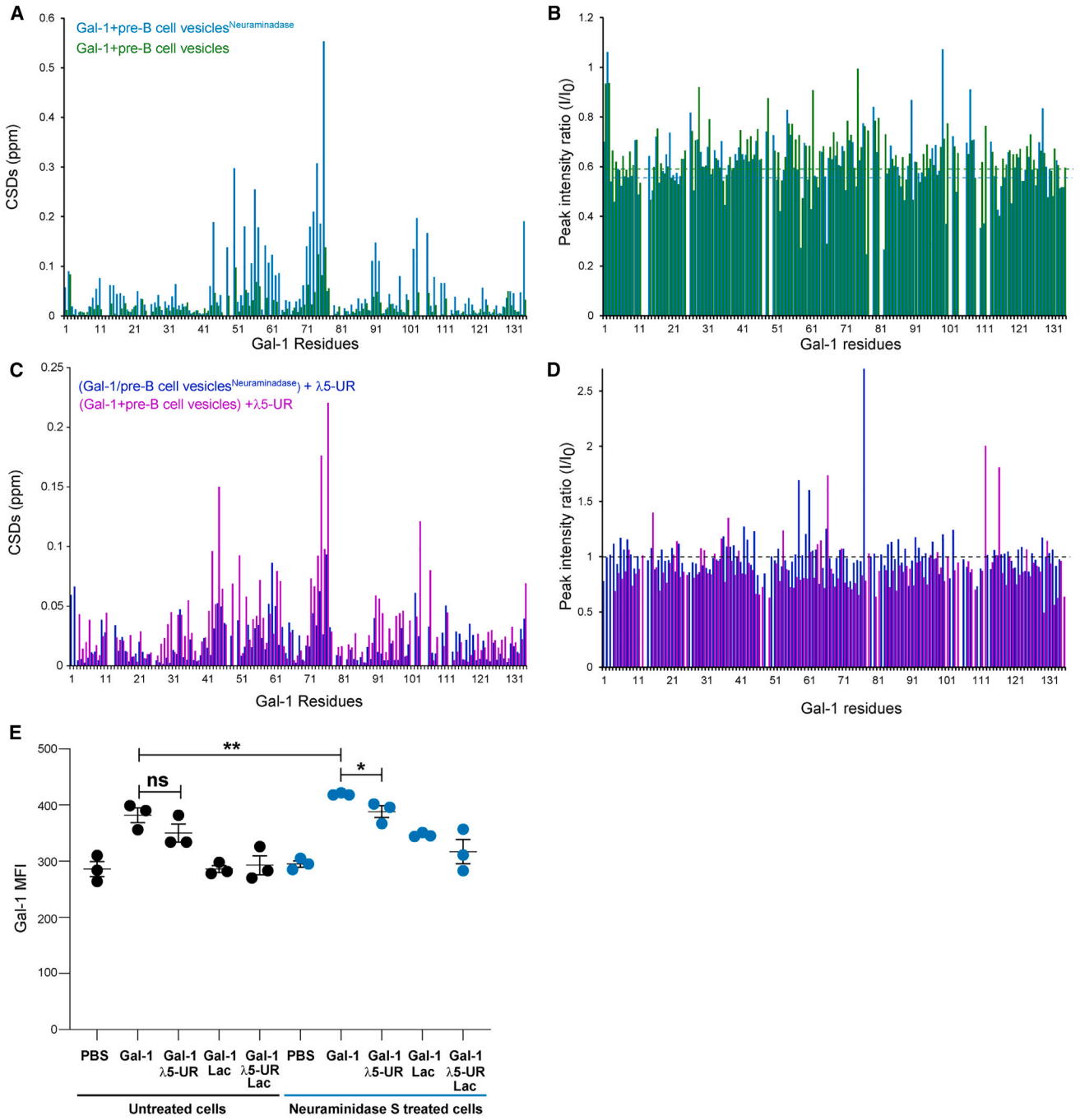

Figure 3. Removal of α2,3-sialylation changes Gal-1 binding to pre-B cells upon λ5-UR interaction

(A) A histogram showing CSDs of Gal-1 resonances bound to neuraminidase S-treated (cyan bars) and -untreated (green bars) pre-B cell vesicles.

(B) Normalized peak intensity ratio analysis (I/I_0) of Gal-1 free relative to Gal-1 bound to neuraminidase S-treated (cyan bars) and -untreated (green bars) pre-B cell vesicles.

(C) CSDs of Gal-1 resonances upon the addition of λ5-UR to Gal-1 bound to neuraminidase S-treated (blue bars) and -untreated (magenta bars) pre-B cell vesicles.

(D) Normalized peak intensity ratio analysis (I/I_0) of Gal-1 bound to neuraminidase S-treated (cyan bars) and -untreated (green bars) pre-B cell vesicles upon the addition of λ5-UR.

(E) Graph representing binding of Gal-1 to pre-B cells (Nalm6), which were incubated at 37°C in the absence or presence of neuraminidase S and then treated as indicated. After treatment, cells were stained with a goat anti-human Gal-1 antibody followed by an anti-goat Alexa Fluor 647 secondary antibody. The mean fluorescence intensity (MFI) was assessed by flow cytometry. Error bars represent SEM from three independent experiments ($n = 3$). Statistical significance was calculated using an unpaired t test. *$p < 0.05$; **$p < 0.01$. ns, not significant.

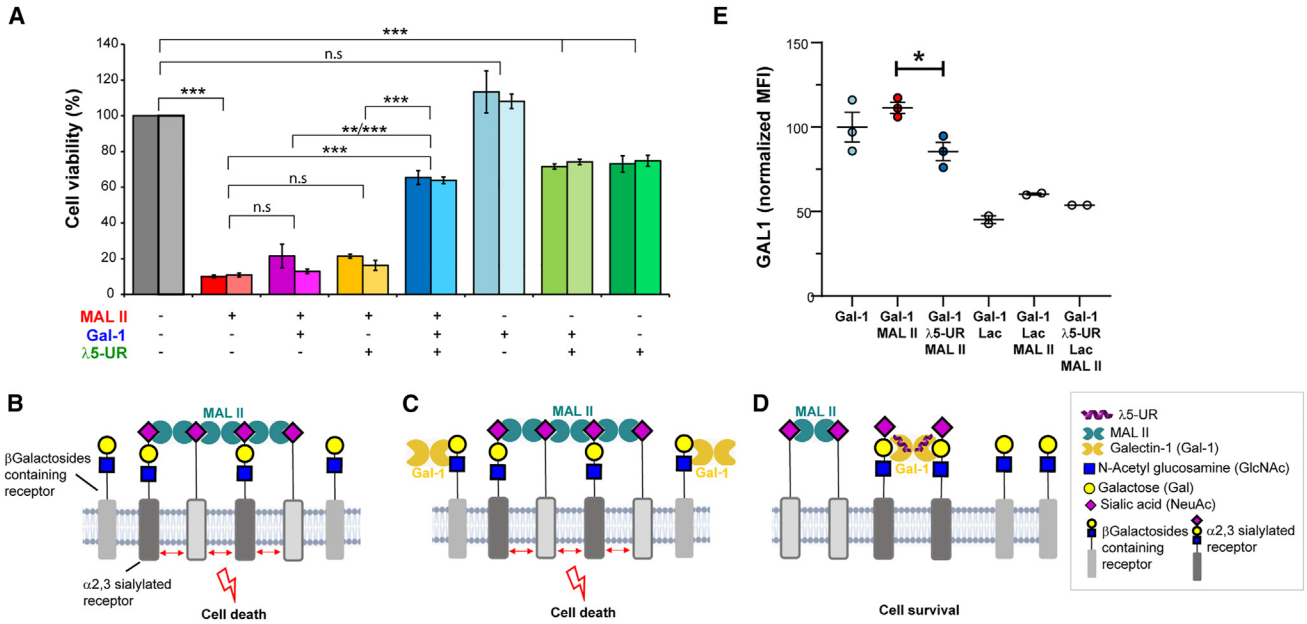

Figure 4. Gal-1 specifically targets α2,3-sialylated glycans at the pre-B cell surface when bound to λ5-UR

(A) Histogram plot showing pre-B cell viability after incubation with MAL II, Gal-1, and λ5-UR as indicated below the histogram. For each condition, two bars are shown: the left bar corresponds to pre-B cell viability evaluated using CellTiter-Glo Luminescent Cell Viability Assay (Promega) and the right bar using the trypan blue exclusion test. Means ± SDs from three independent experiments ($n = 3$) are presented. Each experiment has been performed using three technical replicates. Statistical testing was performed using a Student's t test. Significant differences are represented as $^{*}p < 0.05$, $^{**}p < 0.01$, and $^{***}p < 0.001$. n.s, no significant differences.

(B) Schematic illustrating MAL II-induced pre-B cell death through clustering of α2,3-sialylated receptors.

(C) The presence of Gal-1 does not perturb MAL II interactions and therefore, pre-B cell death.

(D) λ5-UR binding to Gal-1 increases Gal-1 binding to α2,3-sialylated receptors containing β-galactosides, thus perturbing MAL II interactions and allowing pre-B cell survival. Glycans are represented using the symbol nomenclature as indicated.[41]

(E) Pre-B cells (Nalm6) were incubated with Gal-1, λ5-UR, MAL II, and lactose as indicated. After treatment, cells were stained as indicated in Figure 3E. The MFI was assessed by flow cytometry. Error bars represent SEM from three independent experiments ($n = 3$), except for lactose-treated samples, where $n = 2$. Statistical significance was calculated using an unpaired t test. $^{*}p < 0.05$.

Gal-1 interaction is not exclusive to the terminal galactose when bound to λ5-UR (Figures 5E and S7B). In addition, the $^{1}H,^{13}C$-HSQC spectrum of SdiLN showed loss of Gal_A and Gal_B resonances upon the addition of λ5-UR, confirming interaction with both terminal and internal galactose (Figures 5F and 5G). On the Gal-1 side, addition of λ5-UR to the Gal-1/SdiLN complex not only intensified the initial perturbations but also propagated the effect toward CBS subsites B–D, illustrating increased intermolecular contacts between the CBS with the pentasaccharide (Figures 5H, S7C, and S7D). This result is dependent on the presence of the sialic acid since the same molecule unsialylated showed decreased binding to Gal-1 in the presence of λ5-UR.[15] Thus, λ5-UR interaction modifies Gal-1 binding to α2,3-sialylated glycan by allowing additional contacts with the pentasaccharide, including with the internal galactose unit (Figure 5I). This selectivity switch is therefore at the basis of Gal-1 target specificity at the pre-B cell surface.

Gal-1-specific targeting of α2,3-sialylated glycans by λ5-UR is involved in pre-BCR activation

Pre-BCR signaling plays a critical role in regulating the proliferation, differentiation, and survival of pre-B cells.[46] Gal-1 interactions at the pre-B synapse are involved in pre-BCRs clustering, which allows pre-BCR activation and subsequent downstream signaling.[24,28] To test whether the λ5-UR-mediated switch on Gal-1-binding specificity is involved in pre-BCR signaling, we monitored phosphorylation of the S6 ribosomal protein (pS6). Increased phosphorylation of this protein is induced following pre-BCR crosslinking with an antibody specific for the immunoglobulin (Ig) heavy chain (anti-μH; Figure 6A). Using an inhibitor of the central tyrosine kinase SYK, activated downstream of the pre-BCR, decreased pS6 to its unstimulated basal level, confirming that the activation of the S6 ribosomal protein is induced by pre-BCR crosslinking. Similarly, when pre-B cells were co-cultured with stromal cells secreting Gal-1, a significant increase in pS6 was observed, consistent with previous studies and confirming Gal-1 involvement in pre-BCR signaling.[47] Removal of α2,3-sialylated glycans at the surface of pre-B cells using neuraminidase S showed a further increased pS6 level as compared to untreated cells. In both situations, S6 activation is clearly dependent on pre-BCR crosslinking by Gal-1 as it is significantly decreased upon lactose addition. These results suggest that α2,3-sialylated glycans are involved in the regulation of pre-BCR activation. Specifically, they seem to have an inhibitory effect on pre-BCR signaling. Since these glycans are specifically targeted by Gal-1 upon λ5-UR interaction, we then incubated

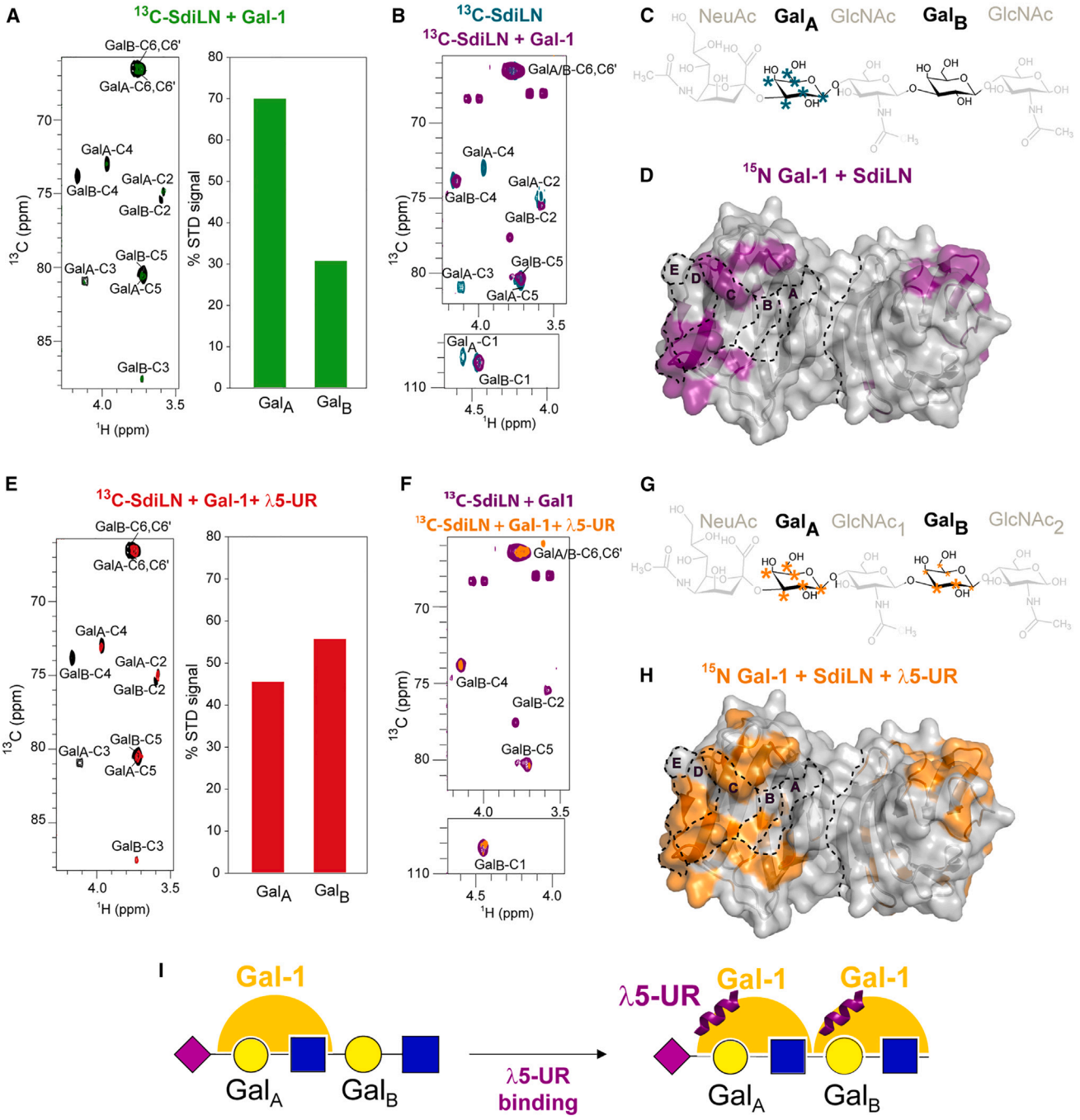

Figure 5. λ5-UR binding to Gal-1 induces enhanced and additional intermolecular contacts with SdiLN

(A) $^{1}H,^{13}C$ STD-HSQC spectrum (left) of 1 mM SdiLN ^{13}C-labeled on galactose moieties in the presence of 10 μM Gal-1. Contribution to Gal-1 binding for each galactose as a percentage of the total STD signal observed is shown (right).

(B) Overlay of $^{1}H,^{13}C$ HSQC of labeled SdiLN (teal) and SdiLN in the presence of an equimolar amount of Gal-1 (purple) showing peaks disappearing and new peaks appearing.

(C) Variations observed in (B) are reported on the SdiLN chemical structure with unlabeled moieties grayed out. Teal stars indicate SdiLN C-H groups for which resonances disappear upon Gal-1 binding.

(D) Chemical shift perturbations observed on $^{1}H,^{15}N$ HSQC spectrum of Gal-1 after the addition of SdiLN are reported on Gal-1 homodimer surface structure. CBS subsites are framed and labeled A–E.

(E–H) Same as in (A)–(D) but after the addition of λ5-UR. (E) $^{1}H,^{13}C$ STD-HSQC spectrum (left) of 1 mM SdiLN ^{13}C-labeled on galactose moieties in the presence of 10 μM Gal-1 and 45 μM λ5-UR. Contribution to Gal-1 binding for each galactose as a percentage of the total STD signal observed is shown (right). (F) Overlay of $^{1}H,^{13}C$ HSQC of labeled SdiLN bound to Gal-1 (purple) and after the addition of λ5-UR (orange). Peaks disappearing or showing decreased intensity are labeled

(legend continued on next page)

the pre-B/stromal cells co-cultures with λ5-UR peptide. The peptide will compete with the pre-BCRs for Gal-1 interaction, which will allow the targeting of α2,3-sialylated receptors by Gal-1 but not their recruitment close to the pre-BCRs. Remarkably, increased pre-BCR activation was observed. This effect is dependent on the presence of α2,3-sialylated glycans, as neuraminidase treatment abolished the λ5-UR effect on the pS6 level. In conclusion, these results demonstrate that within the pre-B synapse, λ5-UR-mediated targeting of Gal-1 interactions toward α2,3-sialylated glycans is involved in the regulation of pre-BCR activation by attenuating downstream signaling.

DISCUSSION

Over the past several decades, many cellular activities have been ascribed to galectins.[4] Such a wide range of functions in so many cell types and environments have induced many laboratories to develop methodologies to understand the varied and intricate roles played by these ubiquitous lectins. While many of the experiments developed provide evidence and enable visualization for galectin-glycoprotein lattices on cell surfaces,[48,49] further studies were needed to understand the galectins' structural features regulating lattice assembly/disassembly at the cellular level. Here, we directly examined the structural properties of Gal-1 binding to native membranes by combining solution-state NMR spectroscopy to the preparation of pre-B and stromal membrane vesicles. Importantly, we could demonstrate that Gal-1 binding to its physiological cellular ligands involves long-range effects throughout the CRD beyond the canonical CBS limits.

Remarkably, our NMR approach allowed us to address how Gal-1 is able to decode the glycome of pre-B cells. Given the abundance of β-galactosides on the cell in the form of glycoproteins and surface glycolipids, one would expect that galectin-glycoconjugate lattice translates into a large heterogeneous complex on the surface of cells. Conversely, this lectin is able to crosslink a single species of glycoproteins to form a uniform lattice.[49–51] Here, we demonstrate that Gal-1 is able to achieve target specificity at the pre-B cell surface through a direct interaction with a non-glycosylated protein domain of the pre-BCR, λ5-UR. This interaction allows Gal-1 to interact with α2,3-sialylated glycoconjugates. Sialic acids are ubiquitously and abundantly found on the surface of all human cells as the terminating sugar in glycolipids (gangliosides) and glycoproteins (complex N-glycans and mucin-type O-linked glycans). Moreover, sialic acids have been shown to play essential roles in immunological processes and, in particular, during BCR signaling.[40,52–55] In this context, the α2,6-sialylated CD22 receptor, which is a lectin recognizing α2,6-sialylated glycoreceptors, is recruited close to the BCR and inhibits its downstream signaling. The objective of this control is to prevent inadvertent activation to weak signals that could be considered a form of self-recognition and/or unwanted B cell responses under the appropriate circumstances.[55] Our results suggest that Gal-1 bound to λ5-UR helps in the recruitment of α2,3-sialylated receptors at the pre-B synapse. Importantly, we showed that the recruited co-receptors play a modulatory role on pre-BCR activation since removal of α2,3-sialylated glycans results in increased pre-BCR-dependent signaling (Figure 6A). Therefore, these receptors may operate on pre-BCR signaling similarly to CD22 receptors during BCR signaling. A model of this proposed regulation is shown in Figure 6B. In this model, Gal-1 secreted by stromal cells binds to glycosylated ligands on pre-B and stromal cells but also to the pre-BCR. The resulting interaction network drives pre-BCR relocalization into the synapse and initiates pre-BCR signaling through the phosphorylation of Igα/Igβ intracellular domains.[24] Restricted receptor segregation into membrane microdomains would result in a homogeneous platform suitable for efficient pre-BCR signaling leading to proliferation and survival. In line with this model of pre-BCR activation, it has been previously observed that Gal-1 binding resulted in the formation of large highly immobile pre-BCR aggregates at the pre-B cell surface.[56] Then, changes in Gal-1 specificity upon pre-BCR interaction would promote α2,3-sialylated receptor recruitment close to the pre-BCR. These co-receptors would antagonize pre-BCR signaling by an unknown mechanism, but it could rely on the recruitment of a phosphatase that would dephosphorylate pre-BCRs, leading to signaling inhibition. Of course, the exact mechanism of this inhibition will need further investigation to be unraveled. Overall, our study reveals that the Gal-1/pre-BCR interaction is part of the glycome-decoding mechanism on the surface of pre-B cells and would aim to re-orchestrate receptor localization to ensure cell signaling regulation and proper B cell development.

At the structural level, upon λ5-UR interaction, dynamic fluctuations throughout Gal-1 occur with an overall increased rigidity that locks Gal-1 into a conformation prone to interact with specific glycans and exclude others. This allostery-based mechanism of regulation for Gal-1-glycan interactions leads to the specific selection of α2,3-sialylated glycoconjugates at the pre-B cell surface. Allostery-based phenomena have been previously shown for Gal-1 binding to synthetic inhibitor molecules designed to target Gal-1 interactions.[57–59] In addition, studies on glycan recognition by Gal-1 showed that sugar binding affected residues far from the CBS and described significant changes in the dynamics of the protein, thus demonstrating Gal-1 conformational plasticity and allostery upon glycan interaction.[31] These data, together with our study, emphasize the existence of intramolecular communication pathways encoded within the Gal-1 structure that link glycan binding to protein interaction. Rather than a simple modification of ligand targeting, these dynamic changes result in Gal-1's increasing intermolecular contacts with both terminal and internal galactose within the α2,3-sialylated pentasaccharide SdiLN. Indeed, Gal-1 bound to λ5-UR is

and shown in orange. (G) Variations are reported on the SdiLN chemical structure. Large orange stars indicate SdiLN C-H groups for which resonances disappear upon Gal-1 and λ5-UR binding. Small orange stars indicate groups showing decreased peak intensity. (H) Chemical shift perturbations observed on ^{1}H,^{15}N HSQC spectrum of Gal-1 after the addition of SdiLN and λ5-UR are reported on Gal-1 homodimer surface structure.
(I) Schematic illustrating the Gal-1 selectivity change upon λ5-UR interaction. Without λ5-UR, Gal-1 acts as an exo-type lectin, binding to the terminal galactose. Upon λ5-UR binding, Gal-1 is also able to interact with the internal galactose.

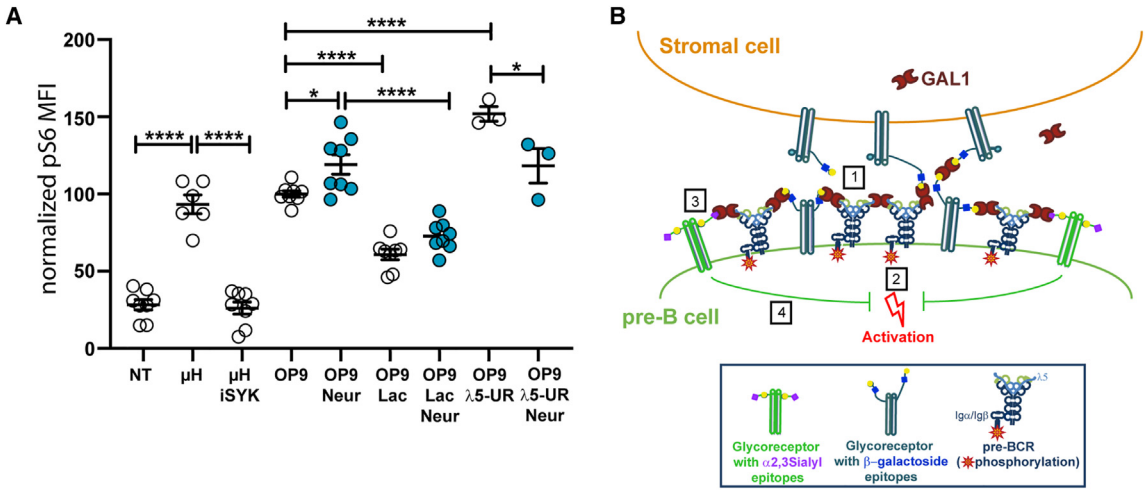

Figure 6. Gal-1 interaction with α2,3-sialylated glycans is involved in pre-BCR activation

(A) Pre-BCR activation of pre-B cells (Nalm6) is induced either through crosslinking with an anti-μH antibody or by performing co-cultures with stromal cells secreting Gal-1 (OP9). Pre-B cells were treated or not with neuraminidase S before their incubation with OP9 stromal cells. The different treatments are presented. After treatment, the pS6 is evaluated by flow cytometry using an anti-pS6 antibody. The MFI has been normalized to 100 on the Nalm-6/OP9 co-culture condition. iSYK, SYK inhibitor; Lac, lactose; λ5-UR, λ5 unique region; μH, anti-μH antibody; Neu, neuraminidase S; NT, untreated. Error bars represent SEM from three to eight independent experiments (n = 3–8). Statistical significance was calculated using an unpaired t test. *$p < 0.05$; **** $p < 0.0001$.

(B) Model for pre-BCR signaling regulation: (1) Gal-1 secreted by stromal cells binds to glycosylated ligands on pre-B and stromal cells but also to the pre-BCR; (2) the resulting interaction network drives pre-BCR relocalization into the synapse and initiates pre-BCR signaling through phosphorylation of Igα/Igβ intracellular domains[24]; (3) then, changes in Gal-1 specificity upon pre-BCR interaction would promote α2,3-sialylated receptor recruitment close to the pre-BCR; (4) these co-receptors would antagonize pre-BCR signaling by a yet-to-be-defined mechanism.

able to interact with terminal and internal galactoses like the tandem-repeat Gal-8.[23] Tandem-repeat galectins (galectins with two CRDs linked by a flexible linker) are known to be more potent in triggering cellular responses[60]; therefore, λ5-UR selectivity-induced change might increase Gal-1 efficiency at the pre-B cell surface through the formation of higher-order multimers as seen for tandem-repeat galectins.[60]

Beyond the pre-BCR case, our results raise a fundamental question: is there a universal mechanism of allosteric modulation of glycan binding that is conserved across all galectins through binding to non-glycosylated protein partners? There is increasing evidence for direct protein interactions with galectins.[16–19] We also demonstrated that CXCL4 interacts with Gal-1 and controls its glycan-binding activities at the base of the immunoregulatory function of galectins.[19] The pre-BCR case and these latter examples involve the three different galectin subfamilies (prototype, chimera, and tandem repeat).[4] Further structural, cellular, and glycomic studies of these new complexes are needed to demonstrate a universal allosteric mechanism of regulation for galectin functions. Moreover, taking into account the involvement of galectins in many crucial pathologies such as cancer[6,61] and inflammation[62] or infection by pathogens,[7] the discovery of this selectivity switch should also increase the potential to develop molecules modulating Gal-1 interactions and function in specific pathological situations.

Limitations of the study

In this study, we demonstrated that pre-BCR binding to Gal-1 fine-tunes its carbohydrate-binding activity. By combining NMR spectroscopy on native membranes with cellular binding assays after different treatments, we identified α2,3-sialylated glycoconjugates as key targeted epitopes. However, the identification of the protein (or lipid) components of these glycoconjugates remains to be unraveled to provide a full understanding of the Gal-1 interaction network at the surface of pre-B cells. Additionally, identifying the recruited α2,3-sialylated receptors would help us to understand how pre-BCR signaling is antagonized inside pre-B cells. Also, changes in Gal-1 binding to stromal cells are observed in the presence of the pre-BCR interacting region, but they could not be investigated further because of the induced strong line broadening in the resulting NMR spectra. These changes might also be involved in pre-BCR signaling regulation by stabilizing the synapse between pre-B and stromal cells, but this remains to be demonstrated.

STAR★METHODS

Detailed methods are provided in the online version of this paper and include the following:

- KEY RESOURCES TABLE
- RESOURCE AVAILABILITY
  - Lead contact
  - Materials availability
  - Data and code availability
- METHOD DETAILS
  - Protein production and purification
  - Peptide synthesis
  - Cell culture
  - Membrane vesicle preparation

- Negative staining electronic microscopy
- PNGase F and O-glycosidase cell treatments
- α2,3-neuraminidase S cell treatment
- GAL1 binding on live pre-B cells
- Pre-B cell activation
- Cell viability assays
- NMR spectroscopy
- General synthesis procedure for N-Acetylneuraminyl-α-2,3-D-Galactopyranosyl-β-1,4-2-N-Acetomido-D-glucopyranosyl-β-1,3-D-Galactopyranosyl-β-1,4-N-Acetyl-D-Glucosamine (SdiLN)
- SdiLN resonance assignment

- QUANTIFICATION AND STATISTICAL ANALYSIS

SUPPLEMENTAL INFORMATION

Supplemental information can be found online at https://doi.org/10.1016/j.celrep.2024.114541.

ACKNOWLEDGMENTS

This work was funded by grants from the Agence Nationale de la Recherche (ANR-16-CE11-0005-01), the Centre National de la Recherche Scientifique, and the Aix-Marseille Université to L.E. The study was also partly supported by grants from Institut National Du Cancer (INCa-2020-096, to S.J.C.M.). This work has benefited from the facilities and expertise of the Platform for Microscopy of the Mediterranean Institute of Microbiology. The authors especially thank Artemis Kostas. We are also grateful to the flow cytometry core facility of the Unité d'Appui à la Recherche Biosit (Rennes).

AUTHOR CONTRIBUTIONS

Conceptualization, P.T., S.J.C.M., and L.E. Investigation, P.T., B.S., A.C., O.B., Q.C., L.G.S., C.S.-K., S.J.C.M., and L.E. Resources, J.R.W. Writing – original draft, L.E. Writing – review & editing, S.J.C.M. and L.E. Visualization, L.E. and S.J.C.M. Supervision, L.E. and S.J.C.M. Funding acquisition, S.J.C.M. and L.E.

DECLARATION OF INTERESTS

The authors declare no competing interests.

Received: November 22, 2022
Revised: May 14, 2024
Accepted: July 9, 2024
Published: July 25, 2024

REFERENCES

1. Varki, A. (2017). Biological roles of glycans. Glycobiology *27*, 3–49. https://doi.org/10.1093/glycob/cww086.
2. Laine, R.A. (1994). A calculation of all possible oligosaccharide isomers both branched and linear yields 1.05 x 10(12) structures for a reducing hexasaccharide: the Isomer Barrier to development of single-method saccharide sequencing or synthesis systems. Glycobiology *4*, 759–767. https://doi.org/10.1093/glycob/4.6.759.
3. André, S., Kaltner, H., Manning, J.C., Murphy, P.V., and Gabius, H.-J. (2015). Lectins: Getting Familiar with Translators of the Sugar Code. Molecules *20*, 1788–1823. https://doi.org/10.3390/molecules20021788.
4. Johannes, L., Jacob, R., and Leffler, H. (2018). Galectins at a glance. J. Cell Sci. *131*, jcs208884. https://doi.org/10.1242/jcs.208884.
5. Leffler, H. (2001). Galectins structure and function–a synopsis. Results Probl. Cell Differ. *33*, 57–83. https://doi.org/10.1007/978-3-540-46410-5_4.
6. Girotti, M.R., Salatino, M., Dalotto-Moreno, T., and Rabinovich, G.A. (2020). Sweetening the hallmarks of cancer: Galectins as multifunctional mediators of tumor progression. J. Exp. Med. *217*, e20182041. https://doi.org/10.1084/jem.20182041.
7. Vasta, G.R. (2020). Galectins in Host–Pathogen Interactions: Structural, Functional and Evolutionary Aspects. In Lectin in Host Defense against Microbial Infections Advances in Experimental Medicine and Biology, S.-L. Hsieh, ed. (Springer), pp. 169–196. https://doi.org/10.1007/978-981-15-1580-4_7.
8. Nio-Kobayashi, J., and Itabashi, T. (2021). Galectins and Their Ligand Glycoconjugates in the Central Nervous System Under Physiological and Pathological Conditions. Front. Neuroanat. *15*, 767330. https://doi.org/10.3389/fnana.2021.767330.
9. Wan, L., Hsu, Y.-A., Wei, C.-C., and Liu, F.-T. (2021). Galectins in allergic inflammatory diseases. Mol. Aspects Med. *79*, 100925. https://doi.org/10.1016/j.mam.2020.100925.
10. van der Hoeven, N.W., Hollander, M.R., Yıldırım, C., Jansen, M.F., Teunissen, P.F., Horrevoets, A.J., van der Pouw Kraan, T.C.T.M., and van Royen, N. (2016). The emerging role of galectins in cardiovascular disease. Vascul. Pharmacol. *81*, 31–41. https://doi.org/10.1016/j.vph.2016.02.006.
11. Sethi, A., Sanam, S., and Alvala, M. (2021). Non-carbohydrate strategies to inhibit lectin proteins with special emphasis on galectins. Eur. J. Med. Chem. *222*, 113561. https://doi.org/10.1016/j.ejmech.2021.113561.
12. Bertuzzi, S., Quintana, J.I., Ardá, A., Gimeno, A., and Jiménez-Barbero, J. (2020). Targeting Galectins With Glycomimetics. Front. Chem. *8*, 593. https://doi.org/10.3389/fchem.2020.00593.
13. Laaf, D., Bojarová, P., Elling, L., and Křen, V. (2019). Galectin–Carbohydrate Interactions in Biomedicine and Biotechnology. Trends Biotechnol. *37*, 402–415. https://doi.org/10.1016/j.tibtech.2018.10.001.
14. Brewer, C., Miceli, M.C., and Baum, L.G. (2002). Clusters, bundles, arrays and lattices: novel mechanisms for lectin–saccharide-mediated cellular interactions. Curr. Opin. Struct. Biol. *12*, 616–623. https://doi.org/10.1016/S0959-440X(02)00364-0.
15. Bonzi, J., Bornet, O., Betzi, S., Kasper, B.T., Mahal, L.K., Mancini, S.J., Schiff, C., Sebban-Kreuzer, C., Guerlesquin, F., and Elantak, L. (2015). Pre-B cell receptor binding to galectin-1 modifies galectin-1/carbohydrate affinity to modulate specific galectin-1/glycan lattice interactions. Nat. Commun. *6*, 6194. https://doi.org/10.1038/ncomms7194.
16. Advedissian, T., Proux-Gillardeaux, V., Nkosi, R., Peyret, G., Nguyen, T., Poirier, F., Viguier, M., and Deshayes, F. (2017). E-cadherin dynamics is regulated by galectin-7 at epithelial cell surface. Sci. Rep. *7*, 17086. https://doi.org/10.1038/s41598-017-17332-y.
17. Daley, D., Mani, V.R., Mohan, N., Akkad, N., Ochi, A., Heindel, D.W., Lee, K.B., Zambirinis, C.P., Pandian, G.S.B., Savadkar, S., et al. (2017). Dectin 1 activation on macrophages by galectin 9 promotes pancreatic carcinoma and peritumoral immune tolerance. Nat. Med. *23*, 556–567. https://doi.org/10.1038/nm.4314.
18. Eckardt, V., Miller, M.C., Blanchet, X., Duan, R., Leberzammer, J., Duchene, J., Soehnlein, O., Megens, R.T., Ludwig, A.-K., Dregni, A., et al. (2020). Chemokines and galectins form heterodimers to modulate inflammation. EMBO Rep. *21*, e47852. https://doi.org/10.15252/embr.201947852.
19. Sanjurjo, L., Schulkens, I.A., Touarin, P., Heusschen, R., Aanhane, E., Castricum, K.C.M., De Gruijl, T.D., Nilsson, U.J., Leffler, H., Griffioen, A.W., et al. (2021). Chemokines modulate glycan binding and the immunoregulatory activity of galectins. Commun. Biol. *4*, 1415–1425. https://doi.org/10.1038/s42003-021-02922-4.
20. Matteucci, C., Nepravishta, R., Argaw-Denboba, A., Mandaliti, W., Giovinazzo, A., Petrone, V., Balestrieri, E., Sinibaldi-Vallebona, P., Pica, F., Paci, M., and Garaci, E. (2023). Thymosin α1 interacts with Galectin-1 modulating the β-galactosides affinity and inducing alteration in the biological activity. Int. Immunopharmacol. *118*, 110113. https://doi.org/10.1016/j.intimp.2023.110113.
21. Gauthier, L., Rossi, B., Roux, F., Termine, E., and Schiff, C. (2002). Galectin-1 is a stromal cell ligand of the pre-B cell receptor (BCR) implicated in

synapse formation between pre-B and stromal cells and in pre-BCR triggering. Proc. Natl. Acad. Sci. USA *99*, 13014–13019. https://doi.org/10.1073/pnas.202323999.

22. Nagae, M., and Yamaguchi, Y. (2014). Three-Dimensional Structural Aspects of Protein–Polysaccharide Interactions. Int. J. Mol. Sci. *15*, 3768–3783. https://doi.org/10.3390/ijms15033768.
23. Moure, M.J., Gimeno, A., Delgado, S., Diercks, T., Boons, G.-J., Jiménez-Barbero, J., and Ardá, A. (2021). Selective 13C-Labels on Repeating Glycan Oligomers to Reveal Protein Binding Epitopes through NMR: Polylactosamine Binding to Galectins. Angew. Chem. Int. Ed. Engl. *60*, 18777–18782. https://doi.org/10.1002/anie.202106056.
24. Rossi, B., Espeli, M., Schiff, C., and Gauthier, L. (2006). Clustering of Pre-B Cell Integrins Induces Galectin-1-Dependent Pre-B Cell Receptor Relocalization and Activation. J. Immunol. *177*, 796–803. https://doi.org/10.4049/jimmunol.177.2.796.
25. Mourcin, F., Breton, C., Tellier, J., Narang, P., Chasson, L., Jorquera, A., Coles, M., Schiff, C., and Mancini, S.J.C. (2011). Galectin-1–expressing stromal cells constitute a specific niche for pre-BII cell development in mouse bone marrow. Blood *117*, 6552–6561. https://doi.org/10.1182/blood-2010-12-323113.
26. Winkler, T.H., and Mårtensson, I.-L. (2018). The Role of the Pre-B Cell Receptor in B Cell Development, Repertoire Selection, and Tolerance. Front. Immunol. *9*, 2423. https://doi.org/10.3389/fimmu.2018.02423.
27. Elantak, L., Espeli, M., Boned, A., Bornet, O., Bonzi, J., Gauthier, L., Feracci, M., Roche, P., Guerlesquin, F., and Schiff, C. (2012). Structural Basis for Galectin-1-dependent Pre-B Cell Receptor (Pre-BCR) Activation. J. Biol. Chem. *287*, 44703–44713. https://doi.org/10.1074/jbc.M112.395152.
28. Espeli, M., Mancini, S.J.C., Breton, C., Poirier, F., and Schiff, C. (2009). Impaired B-cell development at the pre-BII-cell stage in galectin-1–deficient mice due to inefficient pre-BII/stromal cell interactions. Blood *113*, 5878–5886. https://doi.org/10.1182/blood-2009-01-198465.
29. López-Lucendo, M.F., Solís, D., André, S., Hirabayashi, J., Kasai, K., Kaltner, H., Gabius, H.-J., and Romero, A. (2004). Growth-regulatory Human Galectin-1: Crystallographic Characterisation of the Structural Changes Induced by Single-site Mutations and their Impact on the Thermodynamics of Ligand Binding. J. Mol. Biol. *343*, 957–970. https://doi.org/10.1016/j.jmb.2004.08.078.
30. Houzelstein, D., Gonçalves, I.R., Fadden, A.J., Sidhu, S.S., Cooper, D.N.W., Drickamer, K., Leffler, H., and Poirier, F. (2004). Phylogenetic Analysis of the Vertebrate Galectin Family. Mol. Biol. Evol. *21*, 1177–1187. https://doi.org/10.1093/molbev/msh082.
31. Bertuzzi, S., Gimeno, A., Núñez-Franco, R., Bernardo-Seisdedos, G., Delgado, S., Jiménez-Osés, G., Millet, O., Jiménez-Barbero, J., and Ardá, A. (2020). Unravelling the Time Scale of Conformational Plasticity and Allostery in Glycan Recognition by Human Galectin-1. Chem. Eur J. *26*, 15643–15653. https://doi.org/10.1002/chem.202003212.
32. Ermakova, E., Miller, M.C., Nesmelova, I.V., López-Merino, L., Berbís, M.A., Nesmelov, Y., Tkachev, Y.V., Lagartera, L., Daragan, V.A., André, S., et al. (2013). Lactose binding to human galectin-7 (p53-induced gene 1) induces long-range effects through the protein resulting in increased dimer stability and evidence for positive cooperativity. Glycobiology *23*, 508–523. https://doi.org/10.1093/glycob/cwt005.
33. Nesmelova, I.V., Ermakova, E., Daragan, V.A., Pang, M., Menéndez, M., Lagartera, L., Solís, D., Baum, L.G., and Mayo, K.H. (2010). Lactose Binding to Galectin-1 Modulates Structural Dynamics, Increases Conformational Entropy, and Occurs with Apparent Negative Cooperativity. J. Mol. Biol. *397*, 1209–1230. https://doi.org/10.1016/j.jmb.2010.02.033.
34. Chien, C.-T.H., Ho, M.-R., Lin, C.-H., and Hsu, S.-T.D. (2017). Lactose Binding Induces Opposing Dynamics Changes in Human Galectins Revealed by NMR-Based Hydrogen–Deuterium Exchange. Molecules *22*, 1357. https://doi.org/10.3390/molecules22081357.
35. Romero, J.M., Trujillo, M., Estrin, D.A., Rabinovich, G.A., and Di Lella, S. (2016). Impact of human galectin-1 binding to saccharide ligands on dimer dissociation kinetics and structure. Glycobiology *26*, 1317–1327. https://doi.org/10.1093/glycob/cww052.
36. Ishima, R., and Torchia, D.A. (2000). Protein dynamics from NMR. Nat. Struct. Biol. *7*, 740–743. https://doi.org/10.1038/78963.
37. Thijssen, V.L.J.L., Postel, R., Brandwijk, R.J.M.G.E., Dings, R.P.M., Nesmelova, I., Satijn, S., Verhofstad, N., Nakabeppu, Y., Baum, L.G., Bakkers, J., et al. (2006). Galectin-1 is essential in tumor angiogenesis and is a target for antiangiogenesis therapy. Proc. Natl. Acad. Sci. USA *103*, 15975–15980. https://doi.org/10.1073/pnas.0603883103.
38. Salomonsson, E., Thijssen, V.L., Griffioen, A.W., Nilsson, U.J., and Leffler, H. (2011). The Anti-angiogenic Peptide Anginex Greatly Enhances Galectin-1 Binding Affinity for Glycoproteins. J. Biol. Chem. *286*, 13801–13804. https://doi.org/10.1074/jbc.C111.229096.
39. Perdicchio, M., Ilarregui, J.M., Verstege, M.I., Cornelissen, L.A.M., Schetters, S.T.T., Engels, S., Ambrosini, M., Kalay, H., Veninga, H., den Haan, J.M.M., et al. (2016). Sialic acid-modified antigens impose tolerance via inhibition of T-cell proliferation and de novo induction of regulatory T cells. Proc. Natl. Acad. Sci. USA *113*, 3329–3334. https://doi.org/10.1073/pnas.1507706113.
40. Courtney, A.H., Puffer, E.B., Pontrello, J.K., Yang, Z.-Q., and Kiessling, L.L. (2009). Sialylated multivalent antigens engage CD22 in trans and inhibit B cell activation. Proc. Natl. Acad. Sci. USA *106*, 2500–2505. https://doi.org/10.1073/pnas.0807207106.
41. Neelamegham, S., Aoki-Kinoshita, K., Bolton, E., Frank, M., Lisacek, F., Lütteke, T., O'Boyle, N., Packer, N.H., Stanley, P., Toukach, P., et al. (2019). Updates to the Symbol Nomenclature for Glycans guidelines. Glycobiology *29*, 620–624. https://doi.org/10.1093/glycob/cwz045.
42. Mayer, M., and Meyer, B. (1999). Characterization of Ligand Binding by Saturation Transfer Difference NMR Spectroscopy. Angew. Chem. Int. Ed. Engl. *38*, 1784–1788. https://doi.org/10.1002/(SICI)1521-3773(19990614)38:12<1784::AID-ANIE1784>3.0.CO;2-Q.
43. Mayer, M., and Meyer, B. (2001). Group Epitope Mapping by Saturation Transfer Difference NMR To Identify Segments of a Ligand in Direct Contact with a Protein Receptor. J. Am. Chem. Soc. *123*, 6108–6117. https://doi.org/10.1021/ja0100120.
44. Stowell, S.R., Dias-Baruffi, M., Penttilä, L., Renkonen, O., Nyame, A.K., and Cummings, R.D. (2004). Human galectin-1 recognition of poly-N-acetyllactosamine and chimeric polysaccharides. Glycobiology *14*, 157–167. https://doi.org/10.1093/glycob/cwh018.
45. Di Virgilio, S., Glushka, J., Moremen, K., and Pierce, M. (1999). Enzymatic synthesis of natural and 13C enriched linear poly-N-acetyllactosamines as ligands for galectin-1. Glycobiology *9*, 353–364. https://doi.org/10.1093/glycob/9.4.353.
46. Übelhart, R., Werner, M., and Jumaa, H. (2016). Assembly and Function of the Precursor B-Cell Receptor. In B Cell Receptor Signaling, T. Kurosaki and J. Wienands, eds. (Springer International Publishing), pp. 3–25. https://doi.org/10.1007/82_2015_475.
47. Pelletier, J., Balzano, M., Destin, J., Montersino, C., Delahaye, M.C., Marchand, T., Bailly, A.-L., Bardin, F., Coppin, E., Goubard, A., et al. (2023). Niche-expressed Galectin-1 is involved in pre-B acute lymphoblastic leukemia relapse through pre-B cell receptor activation. iScience *26*, 106385. https://doi.org/10.1016/j.isci.2023.106385.
48. Lajoie, P., Partridge, E.A., Guay, G., Goetz, J.G., Pawling, J., Lagana, A., Joshi, B., Dennis, J.W., and Nabi, I.R. (2007). Plasma membrane domain organization regulates EGFR signaling in tumor cells. J. Cell Biol. *179*, 341–356. https://doi.org/10.1083/jcb.200611106.
49. Pace, K.E., Lee, C., Stewart, P.L., and Baum, L.G. (1999). Restricted Receptor Segregation into Membrane Microdomains Occurs on Human T Cells During Apoptosis Induced by Galectin-1. J. Immunol. *163*, 3801–3811.
50. Nguyen, J.T., Evans, D.P., Galvan, M., Pace, K.E., Leitenberg, D., Bui, T.N., and Baum, L.G. (2001). CD45 Modulates Galectin-1-Induced T Cell

Death: Regulation by Expression of Core 2 O-Glycans. J. Immunol. *167*, 5697–5707. https://doi.org/10.4049/jimmunol.167.10.5697.

51. Sacchettini, J.C., Baum, L.G., and Brewer, C.F. (2001). Multivalent Protein−Carbohydrate Interactions. A New Paradigm for Supermolecular Assembly and Signal Transduction. Biochemistry *40*, 3009–3015. https://doi.org/10.1021/bi002544j.
52. O'Keefe, T.L., Williams, G.T., Davies, S.L., and Neuberger, M.S. (1996). Hyperresponsive B Cells in CD22-Deficient Mice. Science *274*, 798–801. https://doi.org/10.1126/science.274.5288.798.
53. Bednar, K.J., Shanina, E., Ballet, R., Connors, E.P., Duan, S., Juan, J., Arlian, B.M., Kulis, M.D., Butcher, E.C., Fung-Leung, W.-P., et al. (2017). Human CD22 Inhibits Murine B Cell Receptor Activation in a Human CD22 Transgenic Mouse Model. J. Immunol. *199*, 3116–3128. https://doi.org/10.4049/jimmunol.1700898.
54. Nanoscale organization and dynamics of the siglec CD22 cooperate with the cytoskeleton in restraining BCR signalling (2016). EMBO J. *35*, 258–280. https://doi.org/10.15252/embj.201593027.
55. Enterina, J.R., Jung, J., and Macauley, M.S. (2019). Coordinated roles for glycans in regulating the inhibitory function of CD22 on B cells. Biomed. J. *42*, 218–232. https://doi.org/10.1016/j.bj.2019.07.010.
56. Erasmus, M.F., Matlawska-Wasowska, K., Kinjyo, I., Mahajan, A., Winter, S.S., Xu, L., Horowitz, M., Lidke, D.S., and Wilson, B.S. (2016). Dynamic pre-BCR homodimers fine-tune autonomous survival signals in B cell precursor acute lymphoblastic leukemia. Sci. Signal. *9*, ra116. https://doi.org/10.1126/scisignal.aaf3949.
57. Dings, R.P.M., Miller, M.C., Nesmelova, I., Astorgues-Xerri, L., Kumar, N., Serova, M., Chen, X., Raymond, E., Hoye, T.R., and Mayo, K.H. (2012). Antitumor Agent Calixarene 0118 Targets Human Galectin-1 as an Allosteric Inhibitor of Carbohydrate Binding. J. Med. Chem. *55*, 5121–5129. https://doi.org/10.1021/jm300014q.
58. Dings, R.P.M., Kumar, N., Miller, M.C., Loren, M., Rangwala, H., Hoye, T.R., and Mayo, K.H. (2013). Structure-Based Optimization of Angiostatic Agent 6DBF7, an Allosteric Antagonist of Galectin-1. J. Pharmacol. Exp. Ther. *344*, 589–599. https://doi.org/10.1124/jpet.112.199646.
59. Dings, R.P.M., Miller, M.C., Griffin, R.J., and Mayo, K.H. (2018). Galectins as Molecular Targets for Therapeutic Intervention. Int. J. Mol. Sci. *19*, 905. https://doi.org/10.3390/ijms19030905.
60. Earl, L.A., Bi, S., and Baum, L.G. (2011). Galectin multimerization and lattice formation are regulated by linker region structure. Glycobiology *21*, 6–12. https://doi.org/10.1093/glycob/cwq144.
61. Elola, M.T., Ferragut, F., Méndez-Huergo, S.P., Croci, D.O., Bracalente, C., and Rabinovich, G.A. (2018). Galectins: Multitask signaling molecules linking fibroblast, endothelial and immune cell programs in the tumor microenvironment. Cell. Immunol. *333*, 34–45. https://doi.org/10.1016/j.cellimm.2018.03.008.
62. Morosi, L.G., Cutine, A.M., Cagnoni, A.J., Manselle-Cocco, M.N., Croci, D.O., Merlo, J.P., Morales, R.M., May, M., Pérez-Sáez, J.M., Girotti, M.R., et al. (2021). Control of intestinal inflammation by glycosylation-dependent lectin-driven immunoregulatory circuits. Sci. Adv. *7*, eabf8630. https://doi.org/10.1126/sciadv.abf8630.
63. Vranken, W.F., Boucher, W., Stevens, T.J., Fogh, R.H., Pajon, A., Llinas, M., Ulrich, E.L., Markley, J.L., Ionides, J., and Laue, E.D. (2005). The CCPN data model for NMR spectroscopy: development of a software pipeline. Proteins *59*, 687–696. https://doi.org/10.1002/prot.20449.
64. Pace, K.E., Hahn, H.P., and Baum, L.G. (2003). Preparation of Recombinant Human Galectin-1 and Use in T-Cell Death Assays. In Methods in Enzymology Recognition of Carbohydrates in Biological Systems, Part B: Specific Applications (Academic Press), pp. 499–518. https://doi.org/10.1016/S0076-6879(03)01075-9.
65. Kodama, H., Nose, M., Niida, S., Nishikawa, S., and Nishikawa, S. (1994). Involvement of the c-kit receptor in the adhesion of hematopoietic stem cells to stromal cells. Exp. Hematol. *22*, 979–984.
66. Hurwitz, R., Hozier, J., Lebien, T., Minowada, J., Gajl-Peczalska, K., Kubonishi, I., and Kersey, J. (1979). Characterization of a leukemic cell line of the pre-B phenotype. Int. J. Cancer *23*, 174–180. https://doi.org/10.1002/ijc.2910230206.
67. Strober, W. (2015). Trypan Blue Exclusion Test of Cell Viability. Curr. Protoc. Immunol. *111*, A3.B.1–A3.B.3. https://doi.org/10.1002/0471142735.ima03bs111.
68. Nesmelova, I.V., Pang, M., Baum, L.G., and Mayo, K.H. (2008). 1H, 13C, and 15N backbone and side-chain chemical shift assignments for the 29 kDa human galectin-1 protein dimer. Biomol. NMR Assign. *2*, 203–205. https://doi.org/10.1007/s12104-008-9121-9.
69. Barbato, G., Ikura, M., Kay, L.E., Pastor, R.W., and Bax, A. (1992). Backbone dynamics of calmodulin studied by 15N relaxation using inverse detected two-dimensional NMR spectroscopy: the central helix is flexible. Biochemistry *31*, 5269–5278. https://doi.org/10.1021/bi00138a005.
70. Kay, L.E., Torchia, D.A., and Bax, A. (1989). Backbone dynamics of proteins as studied by 15N inverse detected heteronuclear NMR spectroscopy: application to staphylococcal nuclease. Biochemistry *28*, 8972–8979. https://doi.org/10.1021/bi00449a003.
71. Farrow, N.A., Muhandiram, R., Singer, A.U., Pascal, S.M., Kay, C.M., Gish, G., Shoelson, S.E., Pawson, T., Forman-Kay, J.D., and Kay, L.E. (1994). Backbone dynamics of a free and phosphopeptide-complexed Src homology 2 domain studied by 15N NMR relaxation. Biochemistry *33*, 5984–6003. https://doi.org/10.1021/bi00185a040.
72. Chen, X., Zhang, W., Wang, J., Fang, J., and Wang, P.G. (2000). Production of α-Galactosyl Epitopes via Combined Use of Two Recombinant Whole Cells Harboring UDP-Galactose 4-Epimerase and α-1,3-Galactosyltransferase. Biotechnol. Prog. *16*, 595–599. https://doi.org/10.1021/bp000052s.
73. Peng, W., Pranskevich, J., Nycholat, C., Gilbert, M., Wakarchuk, W., Paulson, J.C., and Razi, N. (2012). Helicobacter pylori β1,3-N-acetylglucosaminyltransferase for versatile synthesis of type 1 and type 2 poly-LacNAcs on N-linked, O-linked and I-antigen glycans. Glycobiology *22*, 1453–1464. https://doi.org/10.1093/glycob/cws101.
74. Yu, C.-C., Kuo, Y.-Y., Liang, C.-F., Chien, W.-T., Wu, H.-T., Chang, T.-C., Jan, F.-D., and Lin, C.-C. (2012). Site-Specific Immobilization of Enzymes on Magnetic Nanoparticles and Their Use in Organic Synthesis. Bioconjug. Chem. *23*, 714–724. https://doi.org/10.1021/bc200396r.
75. Lee, H.C., Lee, S.-D., Sohng, J.K., and Liou, K. (2004). One-pot enzymatic synthesis of UDP-D-glucose from UMP and glucose-1-phosphate using an ATP regeneration system. J. Biochem. Mol. Biol. *37*, 503–506. https://doi.org/10.5483/bmbrep.2004.37.4.503.

STAR★METHODS

KEY RESOURCES TABLE

REAGENT or RESOURCE	SOURCE	IDENTIFIER
Antibodies		
Human mH chain purified Goat Polyclonal	ThermoFischer	Cat# A18837; RRID: AB_2535614
Human Galectin-1 purified	R&D Systems	Cat#AF1152; RRID: AB_2136626
Goat F(ab')2 IgG (H + L) Alexa Fluor 647 Donkey polyclonal	Jackson ImmunoResearch	Cat#115-606-003; RRID: AB_2338921
Phospho-S6 Ribosomal Protein (Ser235/236) (D57.2.2E) XP® Rabbit mAb Alexa Fluor® 647	Cell Signaling Technology	Cat#4851S; RRID: AB_10695457
Bacterial and Virus Strains		
BL21(DE3)	New England Biolabs	C25271
Chemicals, Peptides, and Recombinant Proteins		
λ5-UR (residue 22–45) peptide	Schafer-N	N/A
λ5-UR-L26A-W30A peptide	Schafer-N	N/A
Anginex peptide	Schafer-N	N/A
Trypsine-EDTA (0.05%) phenol red	ThermoFischer Scientific	25300–054
PBS 1X	ThermoFischer Scientific	20012–027
Lactose	Sigma	L3750-100G
AMMONIUM CHLORIDE (15*N* 99% + 15N)	Eurisotop	NLM-467-10
GLUCOSE-D (U-13C6 99%13C)	Eurisotop	CLM-1396-10
SYTOX Blue	ThermoFisher	Cat# S11348
Human Galectin-1 (Gal-1)	Elantak et al.[27]	N/A
AB8779 inhibitor	AB Science	N/A
PNGase F	New England Biolabs	Cat# P0708S
O-glycosidase	New England Biolabs	Cat# P0733S
Neuraminidase S	New England Biolabs	Cat# P0743L
MAL II unconjugated	Vector Laboratories	Cat# L-1260-2
Critical Commercial Assays		
Pierce BCA protein assay kit	ThermoFischer Scientific	Cat# 23225
PerFix EXPOSE	Beckman Coulter	Cat#B26967
CellTiter-Glo®assay	Promega	Cat# G7570
Experimental Models: Cell Lines		
Nalm6	Cellausorus	CVCL_0092
OP9-shGal1	Espeli et al.[28]	N/A
OP9	RIKEN	N/A
Recombinant DNA		
pQE60-hGal1	lead contact	Elantak et al.[27]
Software and Algorithms		
ccpNMR Anaysis Version 2	Vranken et al.[63]	N/A
PyMol, The PyMOL Molecular Graphics System	Schrödinger, LLC	N/A
DiVa version 9	BD Biosciences	http://www.bdbiosciences.com/
GraphPad Prism version 9.5.0	GraphPad	https://www.graphpad.com/
Dynamic center	Bruker Corporation, USA	N/A

RESOURCE AVAILABILITY

Lead contact

Further information and requests for resources and reagents should be directed to and will be fulfilled by the lead contact, Latifa Elantak (elantak@imm.cnrs.fr).

Materials availability

Any material requests and information should be directed to the lead contact.

Data and code availability

- The data reported in this study are available upon request from the lead contact.
- This paper does not report original code.
- Any additional information required to reanalyze the data reported in this work paper is available from the lead contact upon request.

METHOD DETAILS

Protein production and purification

^{15}N-labeled Gal-1 has been produced and purified as previously described.[64] Protein purity was checked using SDS–polyacrylamide gel electrophoresis.

Peptide synthesis

The λ5-UR (residue 22–45) and λ5-UR-L26A-W30A peptides were chemically synthesized and purchased from Schafer-N, Copenhagen, Denmark.

Cell culture

The murine stromal cell line OP9[65] used in this study corresponds to OP9 cells whose Gal-1 expression was decreased by 75% using a Gal-1-specific shRNA (Thereafter called OP9-shGAL1[28]) were used in the study. The cells were cultivated in MEMα-Glutamax, 20% fetal calf serum (FCS), 100 U.ml−1 penicillin and 100 μg.mL−1 streptomycin. The human leukemic pre-B cell line Nalm6[66] was grown in RPMI, 10% fetal calf serum, 100 U.ml−1 penicillin, 100 μg.mL−1 streptomycin and 50 μM β-mercaptoethanol.

Membrane vesicle preparation

OP9-shGAL1 cells were mechanically detached from the dishes using cell scrapers to avoid the use of trypsine. Nalm6 cells were grown in suspension. Upon centrifugation at 450*g* during 5 min at room temperature, both cell lines were re-suspended with PBS (Phosphate Buffer Saline) 1X (137 mM NaCl pH 7.4, 2.7 mM KCl, 4.3 mM Na_2HPO_4, 1.47 mM KH_2PO_4). Cells were vesiculated by sonication and subsequently centrifuged at 100,000g for 1h at 4°C to collect membrane vesicles. Vesicles were resuspended in 20 mM KPO_4 pH 5.2 buffer. Protein concentration is then estimated using the Pierce BCA protein assay kit.

Negative staining electronic microscopy

Experiments were performed using samples of pre-B or stromal cell vesicles placed on glow-discharged carbon-coated grid during 60 s and the excess solution was removed by touching a piece of filter paper to the side of the grid. After the adsorption of the sample on the support, the grid was washed by being placed on the surface of a drop of deionized water. This step was repeated three times before the grid was blotted dry with filter paper. Three drops of filtered (0.02μm filter) 2% uranyl formate solution were applied on the sample during 3 min for each drop before the excess solution was removed by blotting similarly between each drop application. The grid was then air dried. The uranyl formate being light-sensitive, the filter syringe was wrapped in aluminum foil to reduced light exposition. Images were recorded on an FEI Tecnai 200-kV electron microscope.

PNGase F and O-glycosidase cell treatments

The cells were resuspended in 50 mM sodium phosphate buffer, centrifuged 5 min (450*g*) at room temperature and the supernatant was discarded. This step was repeated twice to allow the removal of the cell media growth. The PNGase F (New England Biolabs) and O-glycosidase (New England Biolabs) enzymes were added (50 000 U and 1 800 000 U, respectively) to 10 million resuspended stromal cells and incubated overnight at 37°C. After centrifugation 5 min at 450 *g* at room temperature, the treated cells were washed twice with PBS buffer. Protein concentration is then estimated before storage at −80°C.

α2,3-neuraminidase S cell treatment

The cells were resuspended in PBS buffer after 5 min centrifugation (450g) at room temperature. This step was repeated twice to eliminate the cell growth media and finally the cells were resuspended in PBS buffer. The enzyme α2,3-neuraminidase S was added (2000U) and the cells were incubated 2 h at 37°C. Two washing steps in PBS were performed before storage at −80°C.

GAL1 binding on live pre-B cells

Nalm6 cells were incubated in PBS with 10 mM HEPES in absence or in presence of 100 U/ml Neuraminidase S (New England Biolabs) during 1 h in an incubator at 37°C and 5% CO_2. Human recombinant Gal-1 was added during the last 20 min of incubation at a final concentration of 35 nM in presence or in absence of MALII (70 nM finale), λ5-UR (350 nM finale) and/or Lactose (25 mM finale), as stated in the figures. After extensive washing in PBS and centrifugation 5 min at 400g, cells were then stained with a purified goat anti hGAL1 antibody (R&D Biosystems) followed by an Alexa Fluor 647 F(ab')2 donkey anti goat IgG (H + L) (Jackson ImmunoResearch) and analyzed by flow cytometry. Dead cells were stained with Sytox Blue (Thermo). FACS acquisition was performed on a Fortessa X20 (BD Biosciences). Data were analyzed using DiVa Version 9 (BD Biosciences).

Pre-B cell activation

Pre-BCR activation of Nalm6 in co-culture with OP9 cells was performed as follows. Nalm6 were starved 60 min in RPMI 0.2% FCS, HEPES 10 mM in absence or in presence of Neuraminidase S (New England Biolabs) at a finale concentration of 100 U/ml. Cells were then immediately transferred on OP9 cells together with 25 mM Lactose or 350 nM λ5-UR, as stated in the corresponding figures, and incubated 90 min at 37°C, 5% CO_2. As a control of pre-BCR activation, starved Nalm6 cells were incubated 15 min with 10 mg/mL goat anti human muH chain (Thermo Fisher) alone or together with 1 mM of the SYK tyrosine kinase inhibitor AB8779 (kind gift from AB Science). The analysis of pre-BCR activation was performed by using the anti phospho-S6 Ribosomal Protein Alexa Fluor 647 (clone D57.2.2E; Cell Signaling Technology) with the PerFix EXPOSE Kit (Beckman Coulter) following the manufacturer instructions. The analysis was performed by flow cytometry.

Cell viability assays

Before treatments, cells were starved with RPMI 0.5% FCS, 100 $U.ml^{-1}$ penicillin and 100 μg mL^{-1} streptomycin during 1h30 at 37°C, 5% CO_2. After two washes with cold PBS, 1.10^6 cells were treated with 10 μg/mL MAL II lectin (Eurobio, L-1260-2) alone or with 10 μg/mL Galectin-1 or with 10 μg/mL Galectin-1 and 100 μg/mL λ5-UR peptide (Schafer-N) during 30min on ice. Then, cells were centrifugated 5 min, 450 g at 4°c and the pellet was resuspended with cold PBS. Pre-B Cell viability was assessed using trypan blue dye exclusion test[67] and the CellTiter-Glo assay (Promega, G7570). For the CellTiter-Glo assay, CTG reagent was mixed at a 1:1 volume ratio with cells on a plastic 96-well plate according to the manufacturer's protocol and luminescence measurements were completed using the TECAN (Männedorf, Suisse). Details on statistical tests, parameters and significance cutoffs are listed in figure legends.

NMR spectroscopy

All NMR experiments have been recorded on a 600 MHz Bruker AVANCE III spectrometer equipped with a TCI cryoprobe at 303 K. All samples were in 20 mM phosphate buffer at pH 5.2. All NMR experiments were recorded using 5 mm NMR tubes except experiments on ^{13}C-labelled SdiLN which were recorded using 3 mm NMR tubes. All spectra were analyzed using ccpNMR Analysis software,[63] and the dynamics spectra experiments were analyzed using the Bruker Dynamic Center software.

NMR titrations: The NMR titrations of Gal-1/vesicles interactions were performed using a series of 2D ^1H, ^{15}N HSQC NMR spectra recorded on a sample of purified ^{15}N-labelled Gal-1 at 200 μM concentration and increasing amounts of cellular vesicles. Final titration points for pre-B and stromal cell vesicles correspond to the addition of vesicles containing 2 mg proteins. To obtain this amount of protein 100 million pre-B and 10 million stromal cells have been used. The same series were performed in the presence of 900 μM λ5-UR peptide. NMR data were analyzed using Gal-1 NMR resonance assignment previously published.[68] The chemical shift perturbations for each resonance were calculated using the equation: $\Delta\delta obs = \left[\Delta\delta^2_{HN} + (\Delta\delta^2_N \div 25)\right]^{1/2}$ where $\Delta\delta_{HN}$ and $\Delta\delta_N$ are, respectively, the proton and nitrogen chemical shift variations of each residue.

STD experiments: 2D ^1H-^{13}C STD HSQC experiments were acquired with a saturation time of 2 s with 256 increments of 128 scans each. The STD experiments were performed using 100:1 SdiLN/Gal-1 and 100:1:3 SdiLN/Gal-1/λ5-UR molar ratio samples at 1 mM concentration for SdiLN. For 1D and 2D STD spectra the on-resonance irradiation was at 6.7 ppm and the off resonance irradiation at 20 ppm and were performed with a saturation time of 2 s. As for the analysis and quantification of the STD, we proceeded as described in other studies.[23] For each cross peak we calculated the STD signal as follows: $\text{STD signal (as a percentage of saturation)} = (I_{STD} \div I_{STDoff}) \times 100$. For Figures 5A and 5E, the contribution to the STD signals from each galactose has been obtained by the sum of the STD signals from each galactose and represented as a percentage from the total STD signals.

NMR relaxation measurements: Dynamics of ^{15}N-Gal-1 free and bound to λ5-UR peptide or Anginex peptide was obtained using NMR experiments acquired at 60.81 MHz for the ^{15}N frequency. The longitudinal (T_1), transverse (T_2), and ^1H–^{15}N-heteronuclear NOE spin relaxation times for the backbone ^{15}N atoms of Gal-1 free and bound to λ5-UR peptide or Anginex peptide were collected at 303 K using the well-established NMR pulse sequences described previously.[69–71] The T_1 and T_2 relaxation times were measured using the following series of the delays: 10, 20, 50, 100, 200, 300, 400, 600, 800, 1000, 1500 and 2000 ms for T_1 and 17.6, 35.2, 52.8, 70.4, 88.0, 105.6, 123.2, 140.8, 158.4 and 176 ms for T_2. The relaxation rates R1 and R2 were calculated by fitting the decay curves to a two-parameter single exponential decay function using the Bruker software Dynamic center. ^1H-^{15}N heteronuclear NOE were measured from the HSQC and the value were calculated as the peak intensity ratio with or without amide proton saturation.

General synthesis procedure for N-Acetylneuraminyl-α-2,3-D-Galactopyranosyl-β-1,4-2-N-Acetomido-D-glucopyranosyl-β-1,3-D-Galactopyranosyl-β-1,4-N-Acetyl-D-Glucosamine (SdiLN)

Materials. All non-stable isotope labeled nucleotides, nucleotide-sugars, enzymes, and chemicals were purchased from Sigma-Aldrich (St. Louis, MO), unless otherwise stated. Ni-NTA Agarose was purchased from Qiagen (Santa Clarita, CA), and Bio-Gel P2 from Bio-Rad (Hercules, CA). Glucose ($^{13}C_6$, 99%) was purchased from Cambridge Isotope Laboratories (Andover, MA). The enzymes used in the synthesis of SdiLN were prepared according published methods: GalE,[72] HP-39,[73] PmST1.[74] The UDP-Glucose ($^{13}C_6$, 99%) was prepared by previously published methods.[75]

*D-Galactopyranosyl-β-1,4-N-Acetyl-D-Glucosamine (*Fig. S6a*, compound 2).* To a reaction mixture (400 μL) containing 40 mM N-Acetyl-D-Glucosamine (Fig. S6a, compound 1, 16 μmol), 48 mM UDP-Glc, 20 mM $MnCl_2$ in 100 mM Sodium Cacodylate Buffer (pH 7.5), β4GalT1 (1 U) and GalE (10 U) were added and incubated overnight at 37°C. The completed reaction, as evident by TLC, was centrifuged and the supernatant subjected to gel filtration on Bio-Gel P-2 (1 × 120 cm column, in 100 mM NH_4HCO_3 solution). Fractions containing 2 were combined and lyophilized to produce a white amorphous solid (∼12.8 μmol, ∼80% isolated yield).

*2-Acetomido-D-Glucopyranosyl-β-1,3-D-Galactopyranosyl-β-1,4-N-Acetyl-D-Glucosamine (*Fig. S6a*, compound 3).* To a reaction mixture (640 μL) containing 10 mM of 2 (6.4 μmol), 12 mM UDP-GlcNAc, 25 mM KCl, 20 mM $MgCl_2$, 1 mM DTT, in 100 mM Sodium Cacodylate Buffer (pH 7.5), HP-39 (10 U) was added and incubated overnight at 37°C. The completed reaction, as evident by TLC, was centrifuged and the supernatant subjected to gel filtration on Bio-Gel P-2 (1 × 120 cm column, in 100 mM NH_4HCO_3 solution). Fractions containing 3 were combined and lyophilized to produce a white amorphous solid (∼4.5 μmol, ∼70% isolated yield).

*D-Galactopyranosyl-β-1,4-2-Acetomido-D-glucopyranosyl-β-1,3-D-Galactopyranosyl-b-1,4-N-Acetyl-D-Glucosamine (*Fig. S6a*, compound 4).* To a reaction mixture (100 μL) containing 40 mM of 3 (4 μmol), 48 mM UDP-Glc, 20 mM $MnCl_2$ in 100 mM Sodium Cacodylate Buffer (pH 7.5), β4GalT1 (1 U) and GalE (10 U) were added and incubated overnight at 37°C. The completed reaction, as evident by TLC, was centrifuged and the supernatant subjected to gel filtration on Bio-Gel P-2 (1 × 120 cm column, in 100 mM NH_4HCO_3 solution). Fractions containing 4 were combined and lyophilized to produce a white amorphous solid (∼3.2 μmol, ∼80% isolated yield).

*N-Acetylneuraminyl-α-2,3-D-Galactopyranosyl-β-1,4-2-Acetomido-D-glucopyranosyl-β-1,3-D-Galactopyranosyl-β-1,4-N-Acetyl-D-Glucosamine: SdiLN (*Fig. S6a*, compound 5).* To a reaction mixture (80 μL) containing 20 mM of 4 (1.6 μmol), 24 mM CMP-Neu5Ac, 20 mM $MnCl_2$ in 100 mM Sodium Cacodylate Buffer (pH 7.5), PmST1 (1 U) was added and incubated overnight at 37°C. The completed reaction, as evident by TLC, was centrifuged and the supernatant subjected to gel filtration on Bio-Gel P-2 (1 × 120 cm column, in 100 mM NH_4HCO_3 solution). Fractions containing 5 (SdiLN) were combined and lyophilized to produce a white amorphous solid (∼0.56 μmol, ∼35% isolated yield).

SdiLN resonance assignment

^1H and ^{13}C NMR resonance assignments of SdiLN have been performed using 2D ^1H, ^{13}C HSQC, 2D ^1H, ^{13}C HSQC-TOCSY, 2D ^1H, ^1H-TOCSY, 2D ^1H, ^1H-ROESY and 2D ^1H, ^1H-COSY experiments. A sample of SdiLN with ^{13}C- labeled Galactoses was used for recording 2D ^1H, ^{13}C HSQC and 2D ^1H, ^{13}C HSQC-TOCSY. Chemical shift assignments are reported in Table S1.

QUANTIFICATION AND STATISTICAL ANALYSIS

The number of biological replicates is indicated in the relevant figure legends. Three technical replicates were performed for each measurement. Details on statistical tests, parameters and significance cutoffs are listed in the relevant figure legends. All statistical analyses were performed using GraphPad Prism software, version 9.5.0 (GraphPad). Significance was defined as follows: *, $p < 0.05$; **, $p < 0.01$; ***, $p < 0.001$; ****, $p < 0.0001$.